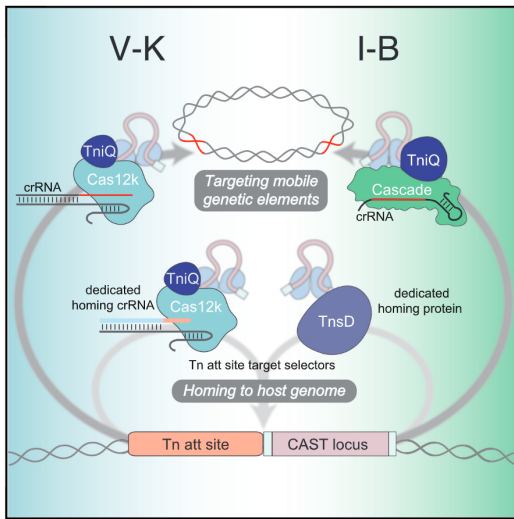


# Dual modes of CRISPR-associated transposon homing

## Graphical abstract



## Authors

Makoto Saito, Alim Ladha, Jonathan Strecker, ..., Han Altae-Tran, Rhiannon K. Macrae, Feng Zhang

## Correspondence

zhang@broadinstitute.org

## In brief

CRISPR-associated transposases (CASTs) undergo RNA-guided transposition. However, they are almost never found in sites targeted by the crRNAs encoded by the cognate CRISPR array, but instead in specific loci on host bacteria genome. This study by Saito et al. reveals two different mechanisms whereby CASTs achieve this “homing” insertion.

## Highlights

- CRISPR-associated transposases (CASTs) use two mechanisms to home to specific locations within the host genome
- Type V-K CAST systems utilize delocalized short crRNA for homing
- Type I-B CAST systems are RNA-guided
- Type I-B CAST systems harbor dedicated attachment site target proteins for homing

Article

# Dual modes of CRISPR-associated transposon homing

Makoto Saito,<sup>1,2,3,4,5,6</sup> Alim Ladha,<sup>1,2,3,4,5,6</sup> Jonathan Strecker,<sup>1,2,3,4,5,6</sup> Guilhem Faure,<sup>1,2,3,4,5,6</sup> Edwin Neumann,<sup>1,2,3,4,5</sup> Han Altae-Tran,<sup>1,2,3,4,5</sup> Rhiannon K. Macrae,<sup>1,2,3,4,5</sup> and Feng Zhang<sup>1,2,3,4,5,7,\*</sup>

<sup>1</sup>Howard Hughes Medical Institute, Cambridge, MA 02139, USA

<sup>2</sup>Broad Institute of MIT and Harvard, Cambridge, MA 02142, USA

<sup>3</sup>McGovern Institute for Brain Research at MIT, Massachusetts Institute of Technology, Cambridge, MA 02139, USA

<sup>4</sup>Department of Brain and Cognitive Sciences, Massachusetts Institute of Technology, Cambridge, MA 02139, USA

<sup>5</sup>Department of Biological Engineering, Massachusetts Institute of Technology, Cambridge, MA 02139, USA

<sup>6</sup>These authors contributed equally

<sup>7</sup>Lead contact

\*Correspondence: [zhang@broadinstitute.org](mailto:zhang@broadinstitute.org)

<https://doi.org/10.1016/j.cell.2021.03.006>

## SUMMARY

Tn7-like transposons have co-opted CRISPR systems, including class 1 type I-F, I-B, and class 2 type V-K. Intriguingly, although these CRISPR-associated transposases (CASTs) undergo robust CRISPR RNA (crRNA)-guided transposition, they are almost never found in sites targeted by the crRNAs encoded by the cognate CRISPR array. To understand this paradox, we investigated CAST V-K and I-B systems and found two distinct modes of transposition: (1) crRNA-guided transposition and (2) CRISPR array-independent homing. We show distinct CAST systems utilize different molecular mechanisms to target their homing site. Type V-K CAST systems use a short, delocalized crRNA for RNA-guided homing, whereas type I-B CAST systems, which contain two distinct target selector proteins, use TniQ for RNA-guided DNA transposition and TnsD for homing to an attachment site. These observations illuminate a key step in the life cycle of CAST systems and highlight the diversity of molecular mechanisms mediating transposon homing.

## INTRODUCTION

CRISPR-Cas systems are adaptive immune systems employed by prokaryotes to defend against foreign genetic elements (Barangou and Horvath, 2017; Marraffini, 2015; Mohanraju et al., 2016). CRISPR-Cas components have been associated with multiple roles beyond adaptive immunity (Faure et al., 2019a, 2019b), however, including guided transposition resulting from the co-option of inactivated Cas effector machinery by transposons (Faure et al., 2019a; Peters et al., 2017). Two distinct subtypes of CRISPR-associated transposon (CAST) systems have been experimentally characterized to date that facilitate RNA-guided targeting of Tn7-like transposons: V-K CAST systems, which utilize Cas12k effectors with naturally inactivated nuclease domains (Strecker et al., 2019), and I-F CAST systems, which utilize Cascade complexes lacking the Cas3 nuclease component (Klompe et al., 2019). In addition, type I-B CAST systems, which also contain components of the Cascade effector in association with Tn7-like transposons, but are extremely rare compared to other CAST systems, have been bioinformatically identified but not yet experimentally characterized (Faure et al., 2019a; Peters et al., 2017).

The prototypical Tn7 transposon from *Escherichia coli* mediates transposition using the core transposase proteins, TnsA, TnsB, and TnsC. These transposase proteins operate in two modes: (1) homing, where TnsABC interact with TnsD, a site-

specific DNA-binding protein, to achieve transposition into the chromosomal *glmS* attachment site (also referred to as the homing site), or (2) mobile element transposition, where TnsABC interact with TnsE, a protein that preferentially directs the transposon to mobile elements including conjugative plasmids (Peters and Craig, 2001; Waddell and Craig, 1988, 1989). These two pathways allow the transposon to safely and efficiently travel from one host to another: after traveling through a mobile element, the TnsD pathway targets a site conserved across hosts to safely home to bacterial chromosomes. CAST systems, which lack *tnsE*, rely on spacers within their CRISPR arrays to achieve targeted transposition (Klompe et al., 2019; Strecker et al., 2019), likely to mobile genetic elements (Faure et al., 2019a, 2019b; Peters et al., 2017). The majority of identified CAST systems in bacterial chromosomes, however, are not located at targets programmed by their CRISPR array, but are rather found next to conserved sequences, including *IMPDH* and SRP RNA in the case of type I-F (Faure et al., 2019a; Peters et al., 2017), suggesting that CAST systems might have an innate homing site. This is also supported by the observation that all known CAST systems identified to date contain *tniQ* (a homolog of *tnsD*), and, in the case of type I-B, two *tniQ* genes. Here, we investigate how CAST systems specifically translocate to bacterial chromosomes and identify two distinct modes of homing in type V-K and type I-B systems involving RNA-mediated and protein-mediated homing, respectively.

### Type V-K CAST systems home via a delocalized CRISPR RNA

We first conducted a bioinformatic survey to determine where type V-K CAST systems are found in bacterial genomes. Comparison of type V-K CAST loci revealed that the transposons preferentially localize to tRNA genes, as previously noted (Klompé et al., 2019), and insertions are typically oriented with Cas12k proximal to the tRNA (46 out of 53 analyzed systems) (Figure 1A). We also observed two insertions neighboring the DNA mismatch repair genes *MutS* and *MutL*, suggesting potential non-random chromosome targets outside of tRNA at a lower frequency. We previously showed that CAST from *Scytonema hofmannii* (ShCAST) can be reconstituted to achieve RNA-guided transposition in *E. coli* (Strecker et al., 2019), and we tested whether it can insert next to the tRNA independent of Cas12k. However, expression of *tnsB*, *tnsC*, and *tniQ* along with the introduction of a pDonor plasmid and a pTarget plasmid containing the re-joined flanking chromosomal sequence did not yield any homing insertions into pTarget as assayed by PCR (Figure S1A). Therefore, we reasoned that another mechanism or protein might be required to direct the ShCAST transposon to its homing target. In the process of analyzing the left end (LE) sequence of ShCAST, we unexpectedly observed a 17-bp motif that perfectly matches the adjacent tRNA-Leu gene. Further analysis revealed the sequence upstream of this motif has partial homology to the CRISPR direct repeat, indicating that this matching sequence could be a delocalized CRISPR RNA (crRNA) (Figure 1B). The delocalized crRNA has a number of mismatches to the direct repeats in the CRISPR array and is irregularly spaced with respect to the array (that is why it was not previously identified), but it does contain 13 nt that perfectly match the 3' end of the canonical direct repeat (Figure S1B). The 17-bp tRNA target sequence is flanked by a GGTT PAM sequence, and the LE of ShCAST is positioned 64 bp downstream of the PAM, consistent with target site requirements observed for crRNA-guided transposition (Strecker et al., 2019). Importantly, we note that a similar discovery of delocalized crRNA for type I-F CAST systems was recently uncovered (Petassi et al., 2020), suggesting a potential common mechanism for CAST homing.

We first tested whether the delocalized crRNA is functional by expressing the natural sequence containing a 37-nt direct repeat and 31-nt spacer (to match the length of crRNA from the adjacent CRISPR array), with only 17 nt of spacer matching the target (Figure 1C), and co-transformed *E. coli* with pHelper, pDonor, and the tRNA-Leu target plasmid. We observed insertions adjacent to the tRNA, and deep sequencing revealed an insertion product with the LE positioned 60- to 70-bp downstream of the spacer (Figure 1D), including the most prominent position at 64 bp that matches the natural insertion found in *S. hofmannii*. We next tested the sequence requirements of the delocalized crRNA by removing 5' and 3' sequences. We found the 5' extension of the 13-nt short direct repeat is dispensable for function whereas loss of the 3' sequence reduced insertion activity (Figure 1C), even though the additional spacer nucleotides do not match the target site. We observed that a minimal crRNA comprised of a 13-nt direct repeat and 17-nt spacer is also capable of homing (Figure 1C). We note that the low inser-

tion activity observed with the delocalized crRNA is likely due to the specific spacer sequence, because targeting PSP1, a previously validated spacer for ShCAST (Strecker et al., 2019), with the same constructs revealed higher activity even though both targets contain the same GGTT PAM (Figure S1C). Interestingly, swapping the delocalized crRNA direct repeat with a canonical direct repeat from the CRISPR array reduced activity between 2- to 10-fold (Figure 1C), suggesting that the delocalized direct repeat might be more efficient at annealing with the tracrRNA and loading into Cas12k.

Only the final 13 nt of the direct repeat is predicted to bind to the tracrRNA (Figure 1E). To determine if the delocalized crRNA represents the absolute minimal targeting requirements for ShCAST, we performed additional truncation analysis of the delocalized crRNA. We were able to delete an additional 3 nt from the 5' end of the direct repeat, however, no deletions to the 17-nt homing spacer were tolerated (Figure S1D). We also tested the insertion activity of ShCAST using a synthetic single guide RNA (sgRNA) containing the 13-nt direct repeat from the delocalized crRNA (Strecker et al., 2019) by deleting different lengths of spacer sequence. We found that 16 nt is both sufficient and near the minimum length required for function (Figures S1E and S1F). Adding double mismatches between the spacer and target revealed that positions 1–16 are sensitive to mutation, while mismatches in positions 17–22 had limited effect on activity (Figure S1G), supporting the idea that only 16 nt of complementary sequence is required for targeted transposition activity. Together these results reveal that the delocalized crRNA is functional for CAST homing and has likely evolved to contain the minimal RNA sequence required for function.

The discovery of a delocalized crRNA in ShCAST led us to examine other type V-K CAST loci, and we were able to identify a delocalized crRNA in 51 out of 53 systems and a matching genomic insertion site in 46 of these 51 systems (Figure 2A; Table S1). Spacers associated with delocalized crRNAs were 16 or 17 nt in length with only a few observed mismatches to their cognate targets, and all delocalized crRNAs contained the terminal 12–14 nt of the canonical direct repeat (Figure S2A). Analysis of tRNA-targeting spacers revealed several frequent sequences including those which target tRNA-Ala and tRNA-Pro (Figure S2B). The location of the delocalized crRNA varied between CAST systems, sometimes occurring as close as 12 bp from the terminal repeat in the array (Figure 2A), and generally with irregular spacing compared to the CRISPR array. This observation suggests that the delocalized crRNAs were not acquired in the same manner as those in the CRISPR array and might be a structural feature of the transposon. Prominent examples of this include the CAST systems from *Cyanobacterium aponinum* IPPAS B-1201 and *Geminocystis* sp. NIES-3709, wherein the delocalized crRNAs are fully embedded within the LE sequence and are over 200 bp from the CRISPR array. Interestingly, delocalized crRNAs are not limited to tRNA targets: the genome insertions adjacent to *MutS*, *MutL*, and *CysH* were also found to match a delocalized crRNA within corresponding transposons (Figure 2A). We identified two additional CAST systems that contain a delocalized crRNA targeting tRNA but lack detectable CRISPR arrays (Figure 2B). It is possible that these two

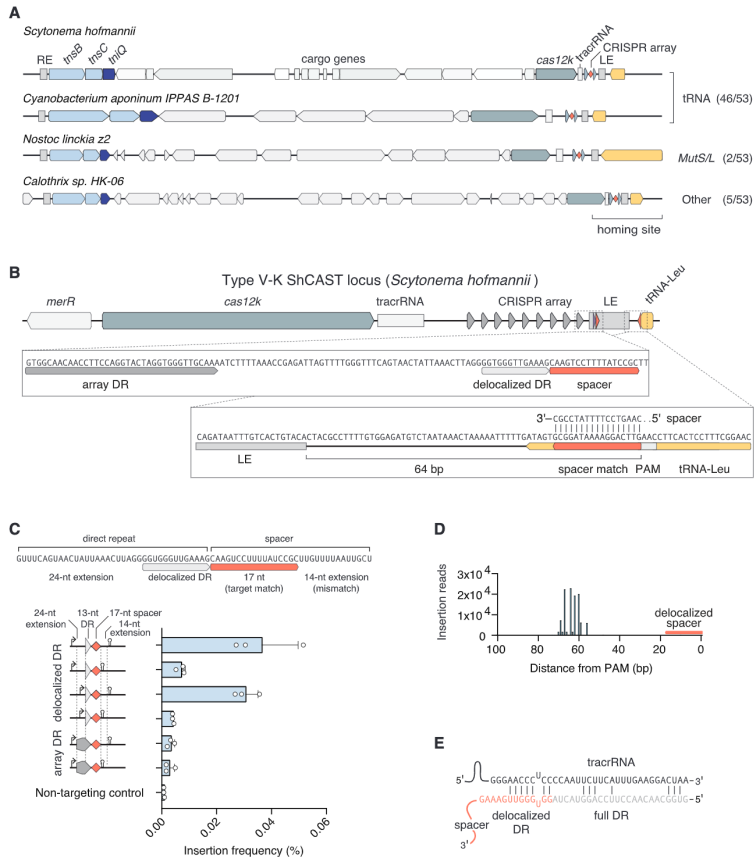


**Figure 1. Homing of type V-K ShCAST is guided by a short, delocalized crRNA**

(A) Representative CAST systems from 53 analyzed loci with their respective homing sites in yellow.  
 (B) Diagram of the delocalized crRNA and corresponding spacer match in downstream tRNA-Leu from *S. hofmannii* CAST.  
 (C) ShCAST homing into a tRNA target plasmid in *E. coli*. Schematic of the natural delocalized crRNA and insertion activity of crRNA variants; promoters and terminators are indicated with an arrow and hairpin, respectively. Data are represented as mean  $\pm$  SD.  
 (D) Deep sequencing of the ShCAST homing insertion product.  
 (E) Schematic representation of the ShCAST tracrRNA interacting with a direct repeat from the canonical CRISPR array.  
 See also Figure S1.

transposons might have the ability to home to conserved bacterial sites but have yet to acquire the ability to target diverse mobile genetic elements or have lost their CRISPR array. Finally, although the locations of delocalized crRNA targets

varied within the cognate genes, because CAST systems insert downstream of the target site, gene integrity was preserved in all cases, with the closest insertions being only 2 bp from the end of the tRNA gene (Figure 2C).



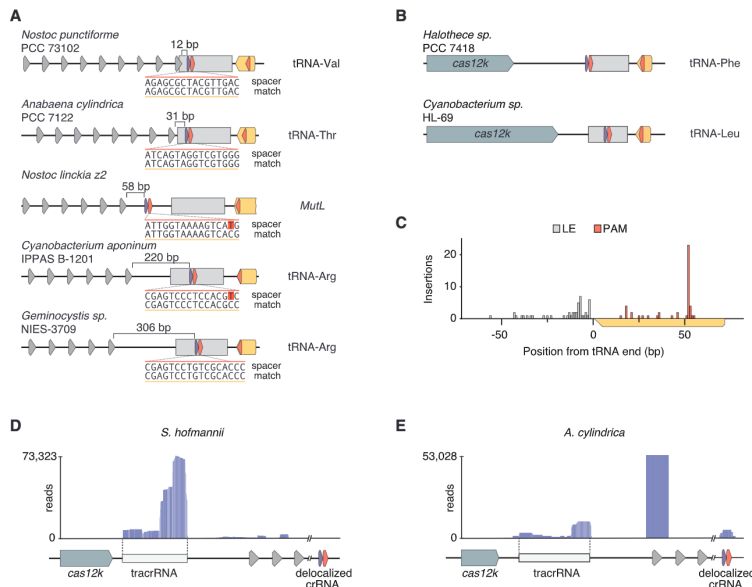


**Figure 2. Diversity of delocalized crRNA across type V-K CAST systems**

(A) Bioinformatic analysis of sequence and distance from the typical CRISPR array of the delocalized crRNA in five CAST systems (see Table S1 for full list). (B) Two type V-K CAST systems (*Halothece* sp. PCC 7418 and *Cyanobacterium* sp. HL-69) that contain a short crRNA targeting the adjacent tRNA, but no detectable CRISPR array. (C) Position of the homing target PAM and corresponding left end (LE) for tRNA-homing CAST systems. (D) RNA sequencing reads from *S. hofmannii* aligned to the delocalized crRNA locus. (E) RNA sequencing reads from *A. cylindrica* aligned to the delocalized crRNA locus. See also Figure S2.

To investigate the identity and expression of the delocalized crRNA in natural cyanobacteria, we analyzed small RNA-sequencing data of two CAST system hosts: *S. hofmannii* and *Anabaena cylindrica* (Strecker et al., 2019). Although we were unable to detect expression of the delocalized crRNA in *S. hofmannii* (Figure 2D), we could readily detect a small RNA species that matched the predicted delocalized crRNA in *A. cylindrica* (Figure 2E). The delocalized crRNA from *A. cylindrica* most commonly contained a 12-nt minimal direct repeat, and ended 2 nt downstream of the 17-nt tRNA spacer (Figure S2C). Based on our experimental characterization of ShCAST, this minimal crRNA contains the required features for RNA-guided transposition and is predicted to be functional. Together, these results suggest that the delocalized crRNA is expressed in some native hosts, but is likely under regulation, and these delocalized crRNAs function to home type V-K CAST systems to conserved locations on bacterial chromosomes.

#### Type I-B systems use two distinct target selector proteins for RNA-guided transposition and homing

To investigate the generality of the RNA-guided homing mechanism to uncharacterized CAST subtypes, we chose to further study the previously identified type I-B CAST system (Faure et al. 2019a; Peters et al. 2017). We searched for delocalized crRNAs in type I-B loci, but we could not detect any crRNAs, canonical or delocalized, that might enable homing. In contrast to type V-K and I-F CAST systems, type I-B subtype 1 (hereafter I-B1) CAST systems uniquely encode two TniQ proteins (Figures 3A and S3A–S3D), and it was previously suggested that one might function with the Cascade complex to provide RNA-guided targeting whereas the other might recognize an attachment site (Peters, 2019; Peters et al., 2017). These two TniQ proteins are more similar to prototypical Tn7 TnsD than those found in other CAST systems, suggesting that they likely evolved from a TnsD Tn7 ancestor (Figures 3B, 3C, S3B, and S3C). Although these TniQ proteins are distinct in their

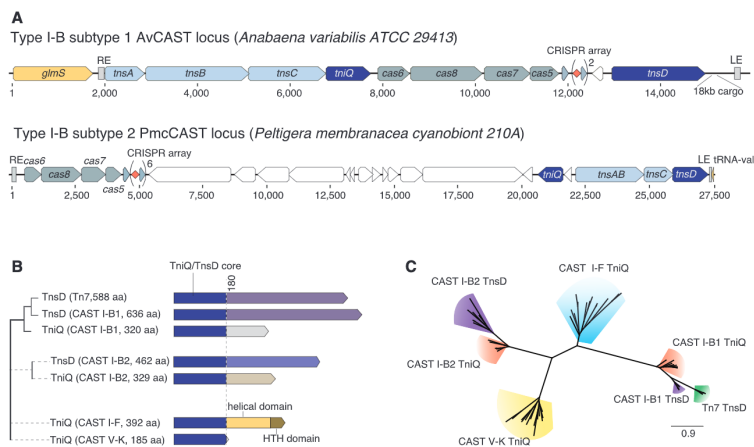


**Figure 3. CAST I-B loci architecture and comparison of the TniQ/TnsD target selectors**

(A) Schematic of the *Anabaena variabilis* ATCC 29413 CAST I-B subtype 1 (I-B1) locus and *Plectonella membranacea cyanobiont* 210A CAST I-B subtype 2 (I-B2) locus containing both Cascade proteins, Tn7-like proteins including TnsD and TniQ target selectors (Figures S3A–S3C). (B) A dendrogram showing the similarity of TniQ/TnsD proteins of Tn7 and CAST I-B1 and I-B2, CAST I-F, and CAST V-K systems (Figures S3B and S3D). Dark purple indicates a similar N-terminal region (TniQ/TnsD core). Light purple indicates similarity between the C-terminal regions of Tn7-TnsD, CAST I-B1 TnsD, and remote similarity with CAST I-B2 TnsD (see Figure S4, S12). Dashed lines indicate boundaries of TniQ/TnsD core. Light and dark yellow colors indicate the protein domains annotated from the CAST I-F TniQ structure (Figure S3D). (C) Phylogenetic tree built with FastTree (WAG model) (Price et al., 2009) from the core region (Figure S3D) of TniQ/TnsD proteins from CAST I-B (TniQ in red; TnsD in purple), Tn7-TnsD (in green), CAST V-K TniQ (in yellow), and CAST I-F TniQ (in cyan). The tree indicates proximity between CAST I-B1 TnsD and Tn7-TnsD and the distinction between CAST I-B1 and CAST I-B2 (Figures S3B and S3D).

C-terminal region, the strong similarity of the longer TniQ to prototypical Tn7 TnsD and the conserved location of type I-B1 CAST loci near *glimS* hint that the longer TniQ may facilitate DNA homing as a site-specific DNA-binding protein. Because of the strong similarity with Tn7 TnsD, we named the longer TniQ as TnsD. We therefore sought to investigate the functions of TnsD and TniQ and determine how I-B1 CAST systems achieve both RNA-guided and homing transposition, focusing on the I-B1 system from *Anabaena variabilis* (ATCC 29413, hereafter AvCAST).

We cloned the nine AvCAST-related genes (*tnsA*, *tnsB*, *tnsC*, *tniQ*, *cas6*, *cas8*, *cas7*, *cas5*, and *tnsD*) into a helper plasmid (pHelper) under IPTG-inducible promoters (Figure 4A; STAR Methods). We cloned the predicted transposon right end (RE) and left end (LE) sequences (Peters et al., 2017) into a donor plasmid (pDonor) with a 0.5-kb cargo sequence. Two direct repeats from the AvCAST CRISPR array with appropriate spacers (i.e., the minimal CRISPR array) were further cloned into pHelper, and crRNA was expressed under an IPTG-inducible promoter. Small RNA-sequencing revealed that transcripts from the minimal CRISPR array are processed into 72-nt mature crRNAs (Figure 4B; Table S2).

Given that AvCAST likely requires a protospacer adjacent motif (PAM) to recognize target DNA, we first targeted a plasmid (pTarget) library containing AvPSP1 flanked by a 6N motif upstream of

the protospacer (Strecker et al., 2019). To clarify the role of AvCAST TniQ and TnsD in RNA-guided transposition, we targeted AvPSP1 with pHelper variants lacking either *tniQ* or *tnsD* (Figure 4A). We detected PAM-RE-cargo-LE (PAM-RL) insertion into the target plasmid by PCR when using pHelpers containing *tniQ*, and furthermore, removal of *tnsD* from the system increased the efficiency of transposition (Figure 4C). The other PAM-LE-cargo-RE (PAM-LR) direction insertions were confirmed by ddPCR (Figure 4D), indicating that the insertion direction is strongly biased (PAM-RL:PAM-LR = 54:1) in contrast to the type I-F system from *Vibrio cholerae* (Klompe et al., 2019). Deep sequencing analysis of the  $\Delta$ *tnsD* condition confirmed the insertion of the RE into pTarget and revealed a preference for 5' AT PAMs (Figure 4E). We next examined the position of the donor in plnsert products relative to AvPSP1, and we detected insertions mainly within an 80- to 86-bp window downstream of the PAM (43–49 bp downstream of the spacer) (Figure 4E). To investigate the exact structure of the plnsert, we performed long read, amplification-free nanopore sequencing. We found only simple insertions generated by type I-B1 AvCAST, whereas type V-K systems showed ~20% cointegrate insertions in this experimental context (Figure 4F, (Strecker et al. 2020)). We also confirmed the existence of target site duplications by Sanger sequencing of individual plnserts (Figure 4G). These results show AvCAST can perform RNA-

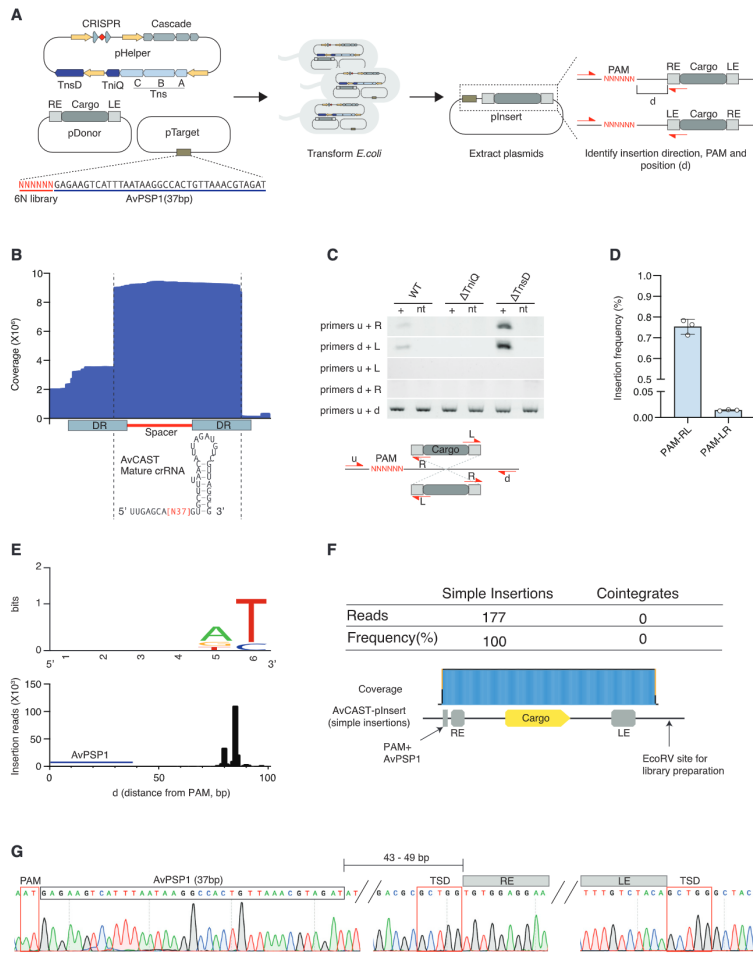


**Figure 4. Characterization of type I-B subtype1 AvCAST**

(A) Schematic of experiment to identify insertion direction, PAM, and insertion position by AvCAST in *E. coli*.  
 (B) RNA sequence reads mapping to the minimal CRISPR array to reveal the mature crRNA sequence of AvCAST.  
 (C) Insertion directionality assayed by diagnostic PCR of plnsert on 6N PAM library plasmid with different primer pairs in  $\Delta$ TniQ or  $\Delta$ TnsD conditions.  
 (D) Quantification of insertion frequency in both directions by ddPCR. Data are represented as mean  $\pm$  SD.  
 (E) Top: PAMs for AvCAST RNA-guided insertions. Bottom: AvCAST RNA-guided insertion positions identified by deep sequencing.  
 (F) Long-read Nanopore sequencing to characterize the structure of plnsert.  
 (G) Sanger sequencing chromatograms of a representative plnsert. PAM, AvPSP1, TSDs, and transposon ends are annotated.  
 See also Figure S4.

guided transposition, and *tniQ* is necessary and sufficient for this activity.

To test whether AvCAST can target bacterial genomic DNA, we picked 36 PAM-containing targets (labeled AvPSP2-37) in *E. coli*. Two separate helper plasmids, pCascade (bearing *cas6*, *cas8*, *cas7*, *cas5*, and the minimal CRISPR array) and pTns (bearing *tnsA*, *tnsB*, *tnsC*, *tniQ*, and *tnsD*) were co-electroporated into *E. coli* with pDonor. Although clear PCR amplicons were detected on the gel at only 10 out of the 36 sites (27.8%) (Figure S4A), 25 sites showed distinguishable signals compared to the no guide control condition by ddPCR (Figure S4B). Further confirmation by deep sequencing revealed that 33 sites showed insertions 70–100 bp downstream of the PAM (33–63 bp downstream of the spacer), as we observed prominent peaks in a 80- to 86-bp window downstream of the PAM (43–49 bp downstream of the spacer) in AvPSP1 targeting (Figure S4C). These results suggest that over 90% of guides are functional, with insertion frequencies between 0.02% and 2.45%. For three representative genomic sites (AvPSP2, AvPSP7, and AvPSP12), we performed tagmentation-based tag integration site sequencing (TTISS) (Schmid-Burgk et al., 2020) to determine the specificity of genome targeting by AvCAST. We observed comparable insertion efficiency with newly constructed heat-sensitive pSC101-donor and pDonor (Figure S4D), and confirmed that 98.8%, 99.8%, and 89.2% of the total insertion reads map to each expected target site (AvPSP2, AvPSP7, and AvPSP12, respectively) by TTISS (Figure S4E). This indicates that AvCAST can be reprogrammed to precisely insert DNA at specific sites in the *E. coli* genome.

Given that *tnsD* is dispensable for RNA-guided transposition, we tested the hypothesis that *tnsD* can mediate homing to the host *glmS* Tn7 attachment site (*attTn7*) (Waddell and Craig, 1989). The native AvCAST contig (CP000117) and two other identical contigs (100% of sequence identity at the nucleotide level) show insertion 5 bp downstream of *glmS* gene stop codon, whereas all other homologous loci from diverse contigs (non-identical) are constantly inserted ~25 bp downstream of the end of *glmS* (Figure S5A). To examine whether AvCAST *tnsD* mediates homing to the *A. variabilis* *glmS* gene (*A.v. glmS*), we generated pTarget(AvCAST) containing the *A.v. glmS* sequence and AvPSP1 flanked by an AT PAM, which we used to assess the transposition efficiency. As we observed for PAM library plasmid targeting, removal of *tnsD* from the system increased insertion frequency at the AvPSP1 site, as quantified by ddPCR (3.0-fold) (Figure 5A). In contrast to RNA-guided transposition, *tniQ* is not necessary for Tn7-like transposition to the *glmS* site. Moreover, removal of *tniQ* from the system increased insertion frequency at the site (16.8-fold) (Figures 5B). We found that the prominent insertion site is 24 bp downstream of *A.v. glmS* gene (Figure 5C), which, although different from the native locus, is similar to other homologous loci. This insertion site was not affected by co-expression of Cascade and TniQ (Figure 5C). We then cloned the downstream region of *glmS* from the native contig into pTarget and repeated the transposition assays to determine if there are additional elements that govern insertion sites. We again observed a prominent insertion site at the canonical Tn7 insertion site, 25 bp downstream of *glmS* (Figure 5C), suggesting there are no additional elements. It is possible the lo-

cus found 5 bp downstream *glmS* in the native contig (CP000117) could result from a 20-bp microdeletion, an idea supported by the lack of target site duplications in this contig.

To obtain additional evidence that this homing transposition is mediated by Tn7-like machinery, we focused on the similarity between *A. variabilis* and *E. coli* *glmS* genes and assessed transposition into target plasmids harboring *glmS* mutations. As expected from the similarity, we observed an insertion 24 bp downstream of the *E. coli* *glmS* gene (Figure S5B). Similarly, expression of all Tn7-like machinery proteins with or without the Cascade complex induced transposition 25 bp downstream of *glmS* in the *E. coli* genome with target site duplications (TSDs) (Figures S5C–S5E). Based on previous findings about *E. coli* *glmS attTn7* (Mitra et al., 2010), we introduced single point mutations at 6 positions previously reported to be important for TnsD attachment and that are conserved between *A. variabilis* and *E. coli* *glmS*. We also constructed an additional 3 variants, two with double mutants and one with all six conserved sites mutated. Each of the six single point mutations in the *A.v. glmS* gene significantly impaired transposition, and both the double point mutants and the sextuple mutant completely abolished it (Figure 5D), suggesting that this homing transposition is achieved through recognition of *attTn7* by AvCAST TnsD.

To further validate these observations, we reconstituted Tn7-like transposition of AvCAST *in vitro* (Bainton et al., 1991) (Figure 5E). As expected, four Tn7 components (*tnsA*, *tnsB*, *tnsC*, and *tnsD*) (Figure S5F) and pDonor resulted in the transposition into a pTarget vector bearing the *E. coli* *glmS* Tn7 attachment site (Figures 5F and 5G).

### A distinct CAST I-B system homes to non-coding RNA sites

We sought to investigate the generalizability of this homing mechanism by considering a second subtype of CAST I-B systems, subtype 2 (hereafter I-B2). In contrast to type I-B1, type I-B2 systems are not found at *glmS* in their native hosts, but are instead found next to tRNA genes (e.g., tRNA-Val and -Ala) (Figures 3A and S3C), similar to type V-K CAST systems. Although type I-B1 and I-B2 share similar Cascade proteins (38% sequence identity, estimated from the concatenation of all Cas protein sequences), their transposon proteins have less than 10% sequence identity (concatenation of all Tn7 protein components). Moreover, although type I-B2 systems contain a TnsC protein and two TniQ proteins (Figure S3C), similar to I-B1 systems, they also harbor a fusion protein of TnsA and TnsB (hereafter TnsAB). Together, these findings suggest Cascade I-B was likely captured by two different transposons in evolutionarily independent events. Given these differences, we sought to determine the mechanisms used by these distinct systems. Among the putative I-B2 CAST systems, we focused on one from *Peltigera membranacea cyanobiont 210A* (PmcCAST) (Figure 3A) to investigate how it homes to tRNA genes. The PmcCAST locus encodes two TniQ proteins, with the larger TniQ protein having a weak but detectable similarity to Tn7 TnsD in its C-terminal region (HHpred probability is 99.26% with a sequence identity of 14%), indicating this protein (hereafter called TnsD) might be the homing selector target protein.

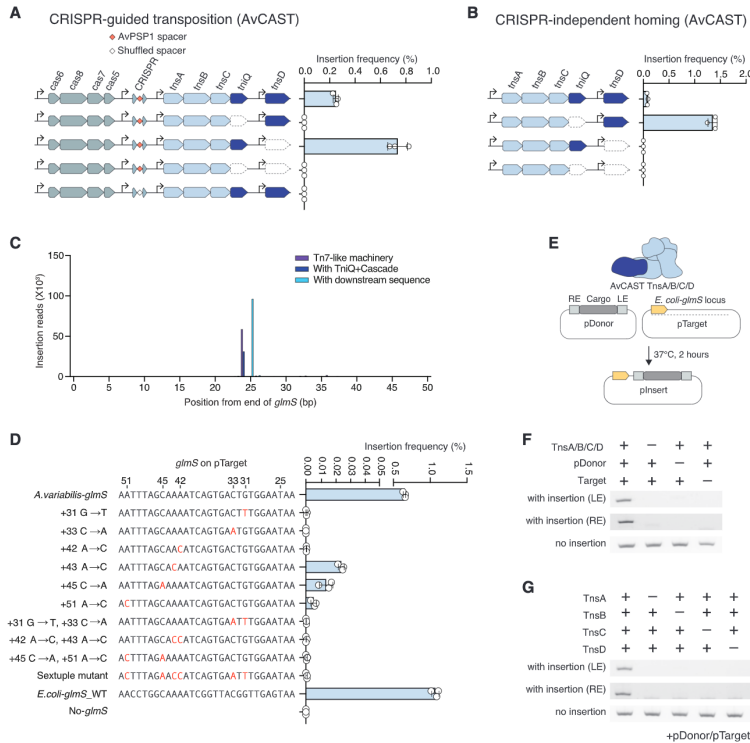


**Figure 5. Homing of AvCAST is mediated through conserved attTn7 recognition by TnsD**

(A) RNA-guided insertion frequency of AvCAST into the pTarget with AvPSP1 and *glmS* gene at each  $\Delta$ TniQ/ $\Delta$ TnsD condition. Data are represented as mean  $\pm$  SD.

(B) Tn7-like machinery-mediated insertion frequency into the pTarget with AvPSP1 and *glmS* gene at each  $\Delta$ TniQ or  $\Delta$ TnsD condition. Data are represented as mean  $\pm$  SD.

(C) AvCAST-mediated single prominent insertion at *glmS* Tn7 attachment site on plasmid identified by deep sequencing. Purple bar indicates the position by Tn7-like machinery (*tnsA*, *tnsB*, *tnsC*, and *tnsD*). Blue bar indicates the position by all AvCAST protein components (Tn7-like machinery + TniQ + Cascade). Light blue bar indicates the insertion position on the plasmid harboring an additional 65 bp downstream sequence of *A. variabilis glmS*.

(D) Tn7-like machinery-mediated insertion frequency of AvCAST into a plasmid bearing the *A. variabilis glmS* gene, a plasmid bearing mutations in the conserved attTn7 site, and a plasmid bearing the *E. coli glmS* gene. The 30 bp of the C terminus of *glmS*, a part of attTn7 identified by a previous study (Mitra et al., 2010), is shown. Base numbering format follows that of the study (end of *glmS* = +23), and reported essential positions for TnsD recognition are shown in red. Data are represented as mean  $\pm$  SD.

(E) Schematic of *in vitro* transposition reactions with purified Tn7-like machinery components of AvCAST.

(F) Tn7-like machinery and donor requirements for *in vitro* transposition on *E. coli glmS* Tn7 attachment site. *plnSert* was detected by PCR for LE and RE junctions.

(G) Tns protein requirements for *in vitro* transposition to the *E. coli glmS* Tn7 attachment site. All reactions contained pDonor and pTarget.

See also Figure S5.

We cloned the eight PmcCAST genes (*tnsAB*, *tnsC*, *tniQ*, *tnsD*, *cas6*, *cas8*, *cas7*, and *cas5*) into a pHelper plasmid with a minimal CRISPR array. Predicted RE and LE sequences with 0.5-kb cargo were further cloned into pDonor. As described above,

we targeted a PmcPSP1-containing 6N PAM library vector to concurrently identify the preferred PAM and insertion position of PmcCAST. We confirmed the expression of a 71-nt mature crRNA by RNA sequencing (Figure S6A; Table S2). Analysis of



PmcCAST plasmids revealed single direction-biased insertions (PAM-RL:PAM-LR = 1:630) within an 83- to 92-bp window downstream of a strong ATG PAM (48–57 bp downstream of spacer) (Figures 6A, S6B, and S6C). In contrast to type I-B1 AvCAST, we found cointegrate insertions by this type I-B2 PmcCAST, whose cointegrate ratio (17%) is comparable to that of type V-K ShCAST (20%) (Streckler et al., 2020) (Figure 6B). We also confirmed the existence of target site duplications of individual plasmids (Figure S6D).

To examine the role of TniQ and TnsD in PmcCAST RNA-guided transposition and homing, we generated pTarget(PmcCAST) containing the host tRNA-Val gene and PmcPSP1 flanked by an ATG PAM. We targeted PmcPSP1 with pHelper and its variants lacking either *tniQ* or *tnsD* (Figure 6C). As with AvCAST, we again found that removal of *tnsD* from the system increased insertion frequency at the PmcPSP1 site, as quantified by ddPCR (14.5-fold) (Figure 6D). Expression of just the Tns proteins by pTns (bearing *tnsAB*, *tnsC*, *tniQ*, and *tnsD*) also induced transposition on pTarget(PmcCAST), and deep sequencing analysis revealed that the prominent insertion site is 31 bp downstream of the tRNA-Val gene, consistent with where PmcCAST is located in the genome (Figures 6E and 6F). For this Tn7-like transposition of PmcCAST to the tRNA-Val homing site, TnsD is essential whereas TniQ is not necessary (Figure 6F). Reconstitution of Tn7-like transposition of PmcCAST *in vitro* (Figure S6E) validated that three protein components (TnsAB, TnsC, and TnsD) and pDonor resulted in the transposition into pTarget(PmcCAST) (Figures 6G and 6H). Thus, although the homing site is different, type I-B2 achieves RNA-guided transposition through the same mechanism used by type I-B1. The detection of high levels of cointegrate plasmids suggests that the TnsAB fusion of PmcCAST does not have the ability to process the 5' ends of the transposon, instead facilitating copy-and-paste transposition into the target site.

## DISCUSSION

The non-random occurrence of CAST insertions within bacterial genomes hints at mechanisms for directing transposition into conserved chromosomal sequences, or homing sites (Figure 7A). Here, we uncover two distinct ways by which CAST systems accomplish this task: V-K systems home using a dedicated delocalized crRNA, primarily to tRNA targets, whereas I-B systems utilize a dedicated *tniQ/tnsD* that mediates homing to *glmS* via direct DNA motif recognition in subtype 1 (similar to the prototypical Tn7) or to various tRNA genes in subtype 2 (Figure 7B). The use of an atypical crRNA expressed from outside of the CRISPR array in type V-K systems reveals remarkable similarity to type I-F CAST systems, which were discovered to also use a non-canonical crRNA to target homing sites (Petassi et al., 2020). This non-canonical crRNA features a variable repeat that is still able to form a hairpin for Cascade recognition and a full length or truncated spacer that can target homing sites despite numerous mismatches with the target. The similarities in these diverse CAST systems highlights the importance of transposon homing, and that in multiple instances, evolution has selected for an RNA-guided solution (Figure S7). These likely ancient homing spacers

have been shaped by evolution from their respective effectors, and shed light on a remarkable ability for target recognition.

The identification of a delocalized homing crRNA across almost all diverse type V-K CAST systems suggests that homing is a critical step in the life cycle of these systems, and the minimal functional length of both the direct repeat and spacer reveals strong pressure to retain effective targeting ability during evolution. The irregular spacing, and often separation, of the delocalized homing crRNA relative to the CRISPR array, and its divergent sequence features, implies different evolutionary constraints and possible acquisition mechanisms imparted by the self-targeting homing spacer and mobile element targeting spacers in the array. Consistent with this idea, we identified two CAST systems that have delocalized crRNA, but no detectable CRISPR arrays (Figure 2B). Why RNA-guided homing is programmed from outside the CRISPR array, and with different sequence features, remains an interesting question. One possibility, as identified in the type I-F systems, is that the delocalized spacer is competent for binding and transposition but does not allow for self-cleavage when in contact with nuclease-competent CRISPR systems (Petassi et al., 2020). However, a search of type V-K CAST systems in fully assembled genomes revealed no co-occurrence of other type V CRISPR systems, indicating that preventing crRNA cross-reactivity may not be a necessary function. We note that more comprehensive co-occurrence analysis is needed once complete genomic information is available for incomplete metagenomic type V-K loci to fully rule out this idea. Alternatively, we hypothesize that the sequence features of the delocalized crRNA could enable protection of the type V-K CAST host from self-cleavage by an ancestral Cas12 nuclease during initial co-option of this CRISPR system by the transposon.

The preference for homing to conserved genes and the ability to insert downstream of the target sequence (e.g., tRNA and *glmS*) allows CAST systems to safely target numerous bacterial species without being deleterious to the host. The use of Cas protein-mediated RNA-guided targeting (that is known to tolerate a small number of mismatches between the RNA guide and its DNA target) of homing sites likely provides some flexibility to recognize variation across bacterial species.

The similarity of CAST I-B1 homing to prototypical Tn7 suggests a close evolutionary relationship and reveals a distinct strategy to integrate safely into chromosomes. Our finding that two separate subtypes of I-B use the same homing mechanism, but target different sites, further supports the notion that type I CRISPR-Cas systems were independently acquired by two distinct Tn7-like transposons.

Our results address a critical gap in our understanding of CAST systems, namely, why they are found at sites not targeted by their CRISPR arrays. We find that while some systems use an RNA-guided homing mechanism, others use a protein-targeted mechanism likely inherited from the transposon. Either one of these mechanisms allows CAST systems to insert themselves into host genomes by targeting well-conserved bacterial genes that serve as safe harbor attachment sites (Figure 7B). Thus, CAST systems seem to utilize two modes of insertion: transposition to mobile elements using RNA-guided targeting and homing using either RNA-guided targeting or the *tniQ/tnsD* pathway, like



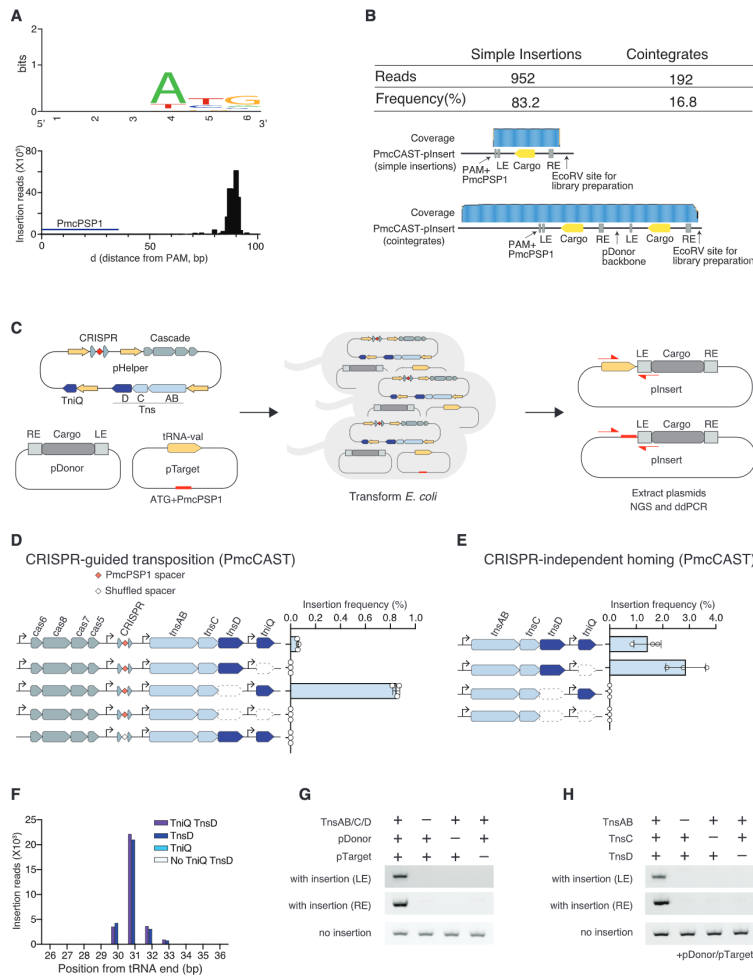


**Figure 6. Type I-B subtype 2 PmcCAST system homes to tRNA-Val**

(A) Top: PAMs for PmcCAST RNA-guided insertions. Bottom: AvCAST RNA-guided insertion positions identified by deep sequencing.

(B) Long-read nanopore sequencing to characterize the structure of plinsert.

(C) Schematic of experiment to compare RNA-guided transposition and homing to tRNA-Val by PmcCAST in *E. coli*.

(D) RNA-guided insertion frequency of PmcCAST into the pTarget with PmcPSP1 and tRNA-Val gene at each  $\Delta$ ttnI or  $\Delta$ ttnD condition. Data are represented as mean  $\pm$  SD.

(E) Tn7-like machinery-mediated insertion frequency of PmcCAST into pTarget at each  $\Delta$ ttnI or  $\Delta$ ttnD condition. Data are represented as mean  $\pm$  SD.

(legend continued on next page)

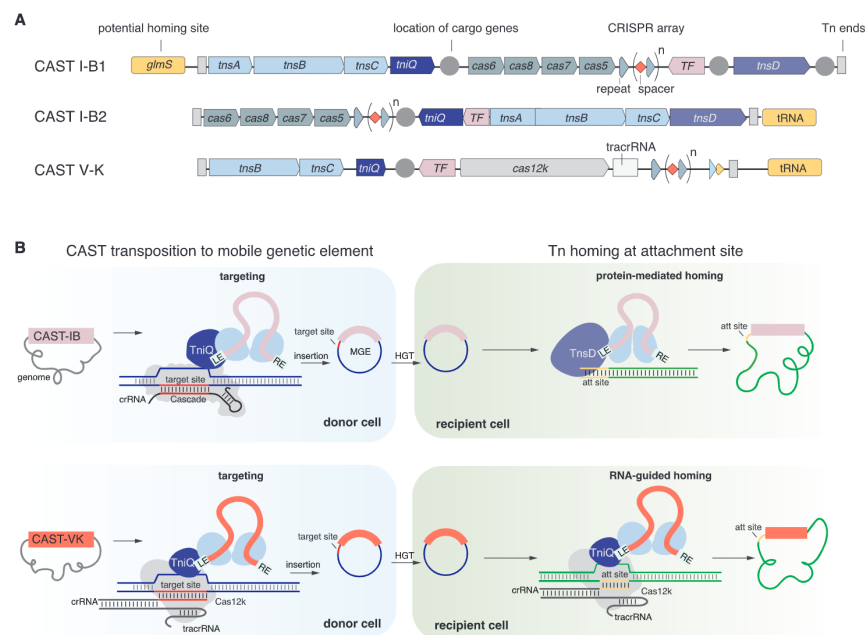


**Figure 7. Models of transposition mechanisms of CAST I-B and CAST V-K systems**

(A) Prototypical loci organization of CAST I-B and CAST V-K systems. The loci are delimited by transposon ends (Tn ends, indicated as light vertical rectangle). Transposon core components (*tnsA*, *tnsB*, and *tnsC* in CAST I-B; *tnsB* and *tnsC* in CAST V-K) are colored in light blue while *tniQ* are indicated in purple with a lighter purple for *tnsD*. Cas components (Cascade and *cas2k*) are shown in gray. Conserved transcription factors (TF) are shown in pink. Locations of cargo genes are indicated with dark gray circles. CRISPR arrays are shown as gray triangles for the repeats and red diamonds for the spacers. The delocalized crRNA is indicated by a lighter triangle (partial repeat) and a truncated red diamond (short spacer). Homing target sites are colored in yellow. Horizontal light gray triangle indicates the *tracrRNA* in the CAST V-K locus. Conserved transcription factors (TF) are shown in light pink.

(B) Models for CAST transposition to mobile element (donor cell in blue) and CAST homing transposition to bacterial chromosome (recipient cell in green). CAST transposition to mobile genetic elements is mediated by the Cas effector machinery (IB Cascade and crRNA or Cas12k, *tracrRNA*, and crRNA; Cas proteins are shown in gray) that recognizes the target site (red) with RNA-guided targeting to insert the transposon using Tn components. *TniQ* may function as an adaptor between Cas machinery and the transposome (Tn core machinery bound to the DNA transposon). The mobile genetic element (MGE) where the transposon has inserted can be horizontally transferred (via horizontal gene transfer (HGT)) to another host, where homing transposition can occur. CAST I-B homing transposition is mediated by *TnsD* (without Cas components), which targets the homing site (light orange) located in the bacterial chromosome (in green). CAST V-K uses a dedicated crRNA to target the homing site.

See also Figure S7.

Tn7 transposons. How these pathways are regulated remains unclear in type V-K and type I-B CAST systems, but it was recently shown for type I-F that conserved transcription factors

are linked to the switch between pathways (Petassi et al., 2020). Consistent with this observation, we can detect conserved transcription factors within CAST V-K and CAST I-B

(F) PmcCAST-mediated prominent insertion at tRNA-Val gene on target plasmid identified by deep sequencing. Purple bar indicates the position by all Tns proteins (*TnsAB*, *TnsC*, *TniQ*, and *TnsD*). Blue bar indicates the position at  $\Delta$ *tniQ* condition. Light blue bar indicates the position at  $\Delta$ *tnsD* condition. White bar indicates the position at  $\Delta$ *tniQ* $\Delta$ *tnsD* conditions.

(G) Tn7-like machinery and donor requirements for *in vitro* transposition on tRNA-Val gene. *inset* was detected by PCR for LE and RE junctions.

(H) Tns protein requirements for *in vitro* transposition on tRNA-Val gene. All reactions contained pDonor and pTarget.

See also Figures S3 and S6.

loci (Figure 7A) that appear to be distinct from cargo genes and could be linked to transposon pathway switching. Further analysis remains to be done to confirm they are pathway regulators. We also note our inability to detect expression of the homing crRNA in the cyanobacteria host *S. hofmannii* hinting at potential regulation. In addition to elucidating homing mechanisms, our work here experimentally characterizes the type I-B CAST systems and demonstrates that both subtypes of I-B CAST systems can transpose via RNA-guided targeting. Importantly, these type I-B CAST systems provide new starting points for developing genome engineering tools for targeted gene insertion in bacterial genomes (Streckler et al., 2019; Klompe et al., 2019; Rubin et al., 2020; Vo et al., 2020) and potential applications in human cells. Collectively, this work advances our understanding of the biology of these systems, highlighting conserved and divergent features, and shedding light on their mechanisms of action.

#### Limitations of study

This study presents two unique targeting mechanisms that enable CAST systems to integrate at their chromosomal attachment sites and reveals two distinct pathways in the CAST life cycle: mobilization and homing. Further work will elucidate how CAST V-K and I-B systems regulate these two pathways. Although we can detect conserved transcription factors in CAST V-K and I-B loci, their role in CAST pathway regulation must be experimentally validated as has been done for CAST I-F systems (Petassi et al., 2020). How spacers are acquired for both mobilization and homing remains a mystery, because the adaptation module is notably absent in CAST loci. Finally, this study adds to the list of potential candidate systems that may be developed for targeted gene insertion applications (along with other CAST V-K and I-F systems) (Streckler et al., 2019; Klompe et al., 2019; Rubin et al., 2020; Vo et al., 2020).

#### STAR★METHODS

Detailed methods are provided in the online version of this paper and include the following:

- [KEY RESOURCES TABLE](#)
- [RESOURCE AVAILABILITY](#)
  - Lead contact
  - Materials availability
  - Data and code availability
- [EXPERIMENTAL MODEL AND SUBJECT DETAILS](#)
  - Bacteria strains
- [METHOD DETAILS](#)
  - Plasmid construction
  - PAM and insert position analysis of AvCAST and PmcCAST
  - *E. coli* Transposition Assays
  - Nanopore sequencing to determine constitutive/replisome transposition
  - Droplet digital PCR (ddPCR) reactions
  - TTSS for AvCAST insertion specificity analysis
  - qPCR Reactions
  - RNA sequencing to recover mature crRNAs

- Purification of Tn7-like machinery components and *in vitro* transposition assays
- Comparative genomic analysis of CAST loci and TriQ/TnsD analysis
- [QUANTIFICATION AND STATISTICAL ANALYSIS](#)

#### SUPPLEMENTAL INFORMATION

Supplemental information can be found online at <https://doi.org/10.1016/j.cell.2021.03.006>.

#### ACKNOWLEDGMENTS

We thank I. Peng, P. Clauer, and J. Kreitz for their assistance with cloning and *E. coli* transposition assays; S. Kannan for her assistance with RNA sequencing analysis of CAST I-B systems; J. Schmid-Burgk and L. Gao for useful discussions; and the entire Zhang laboratory for support and advice. We also thank A. Farina for preparation of reagents. M.S. was supported by a fellowship from the Swiss National Science Foundation, Switzerland, and is currently supported by a Long-Term Fellowship from Human Frontier Science Program. J.S. was supported by a Long-Term Fellowship from the Human Frontier Science Program. F.Z. is supported by the NIH (1DP1-HL141201, R01-HG009761, and RM1-HG006193), the G. Harold and Lella Y. Mathers Foundation, the Edward Mallinckrodt, Jr. Foundation, and Gates Foundation, the Howard Hughes Medical Institute, the Poitras Center for Psychiatric Disorders Research, the Open Philanthropy Project, the Hock E. Tan and K. Lisa Yang Center for Autism Research at MIT, J. and P. Poitras, the Phillips family, and R. Metcalfe.

#### AUTHOR CONTRIBUTIONS

M.S., A.L., J.S., G.F., and F.Z. conceived of the project. M.S. and G.F. contributed equally to the study of the CAST I-B system. A.L. and J.S. contributed equally to the study of the CAST V-K system. M.S., A.L., J.S., and E.N. designed and conducted bacterial and biochemical experiments. M.S., A.L., J.S., and E.N. performed data analysis. G.F. carried out computational and evolutionary analysis of CAST systems. H.A.-T. created a microbial metagenomic and genomic database. F.Z. supervised the research and experimental design. M.S., A.L., J.S., G.F., R.M., and F.Z. wrote and revised the manuscript with input from all authors.

#### DECLARATION OF INTERESTS

The Broad Institute has filed patent applications related to this work. F.Z. is a scientific advisor and cofounder of Editas Medicine, Beam Therapeutics, Pairwise Plants, Arbor Biotechnologies, and Sherlock Biosciences.

Received: November 4, 2020

Revised: January 25, 2021

Accepted: March 2, 2021

Published: March 25, 2021

#### REFERENCES

- Altschul, S.F., Gish, W., Miller, W., Myers, E.W., and Lipman, D.J. (1990). Basic local alignment search tool. *J. Mol. Biol.* 215, 403–410.
- Bainton, R., Gamas, P., and Craig, N.L. (1991). Tn7 transposition *in vitro* proceeds through an excised transposon intermediate generated by staggered breaks in DNA. *Cell* 65, 805–816.
- Barrangou, R., and Horvath, P. (2017). A decade of discovery: CRISPR functions and applications. *Nat. Microbiol.* 2, 17092.
- Callebaut, I., Labesse, G., Durand, P., Poupon, A., Canard, L., Chomilier, J., Henrissat, B., and Mornon, J.P. (1997). Deciphering protein sequence information through hydrophobic cluster analysis (HCA): current status and perspectives. *Cell. Mol. Life Sci.* 53, 621–645.

- Chan, P.P., and Lowe, T.M. (2019). tRNAscan-SE: Searching for tRNA Genes in Genomic Sequences. *Methods Mol. Biol.* 1962, 1–14.
- Eddy, S.R. (2009). A new generation of homology search tools based on probabilistic inference. *Genome Inform* 23, 205–211.
- Faure, G., and Callebaut, I. (2013a). Comprehensive repertoire of foldable regions within whole genomes. *PLoS Comput. Biol.* 9, e1003280.
- Faure, G., and Callebaut, I. (2013b). Identification of hidden relationships from the coupling of hydrophobic cluster analysis and domain architecture information. *Bioinformatics* 29, 1726–1733.
- Faure, G., Shmakov, S.A., Yan, W.X., Cheng, D.R., Scott, D.A., Peters, J.E., Makarova, K.S., and Koonin, E.V. (2019a). CRISPR-Cas in mobile genetic elements: counter-defence and beyond. *Nat. Rev. Microbiol.* 17, 513–525.
- Faure, G., Makarova, K.S., and Koonin, E.V. (2019b). CRISPR-Cas: Complex Functional Networks and Multiple Roles beyond Adaptive Immunity. *J. Mol. Biol.* 431, 3–20.
- Griffiths-Jones, S., Bateman, A., Marshall, M., Khanna, A., and Eddy, S.R. (2003). Rfam: an RNA family database. *Nucleic Acids Res.* 31, 439–441.
- Halpin-Healy, T.S., Klompe, S.E., Sternberg, S.H., and Fernández, I.S. (2020). Structural basis of DNA targeting by a transposon-encoded CRISPR-Cas system. *Nature* 577, 271–274.
- Hyatt, D., Chen, G.-L., Locascio, P.F., Land, M.L., Larimer, F.W., and Hauser, L.J. (2010). Prodigal: prokaryotic gene recognition and translation initiation site identification. *BMC Bioinformatics* 11, 119.
- Petassi, M.T., Hsieh, S.-C., and Peters, J.E. (2020). Guide RNA categorization enables target site choice in Tn7-CRISPR-Cas transposons. *Cell* 183, 1757–1771.
- Vo, P.L.H., Ronda, C., Klompe, S.E., Chen, E.E., Acrece, C., Wang, H.H., and Sternberg, S.H. (2020). CRISPR RNA-guided integrases for high-efficiency and multiplexed bacterial genome engineering. *Nat. Biotechnol.* Published online November 23, 2020. <https://doi.org/10.1038/s41587-020-00745-y>.
- Katoh, K., Kuma, K., Toh, H., and Miyata, T. (2005). MAFFT version 5: improvement in accuracy of multiple sequence alignment. *Nucleic Acids Res.* 33, 511–518.
- Kearse, M., Moir, R., Wilson, A., Stones-Havas, S., Cheung, M., Sturrock, S., Buxton, S., Cooper, A., Markowitz, S., Duran, C., et al. (2012). Geneious Basic: an integrated and extendable desktop software platform for the organization and analysis of sequence data. *Bioinformatics* 28, 1647–1649.
- Keegan, K.P., Glass, E.M., and Meyer, F. (2016). MG-RAST, a Metagenomics Service for Analysis of Microbial Community Structure and Function. *Methods Mol. Biol.* 1399, 207–233.
- Klompe, S.E., Vo, P.L.H., Halpin-Healy, T.S., and Sternberg, S.H. (2019). Transposon-encoded CRISPR-Cas systems direct RNA-guided DNA integration. *Nature* 577, 219–225.
- Leticic, I., and Bork, P. (2007). Interactive Tree Of Life (ITOL): an online tool for phylogenetic tree display and annotation. *Bioinformatics* 23, 127–128.
- Makarova, K.S., Wolf, Y.I., Iranzo, J., Shmakov, S.A., Alkhnbashi, O.S., Brouns, S.J.J., Charpentier, E., Cheng, D., Haft, D.H., Horvath, P., et al. (2020). Evolutionary classification of CRISPR-Cas systems: a burst of class 2 and derived variants. *Nat. Rev. Microbiol.* 18, 67–83.
- Marraffini, L.A. (2015). CRISPR-Cas immunity in prokaryotes. *Nature* 526, 55–61.
- Mitra, R., McKenzie, G.J., Yi, L., Lee, C.A., and Craig, N.L. (2010). Characterization of the TnsD-attTn7 complex that promotes site-specific insertion of Tn7. *Mob. DNA* 1, 18.
- Mohanraju, P., Makarova, K.S., Zetsche, B., Zhang, F., Koonin, E.V., and van der Oost, J. (2016). Diverse evolutionary roots and mechanistic variations of the CRISPR-Cas systems. *Science* 353, aad5147.
- Nawrocki, E.P., and Eddy, S.R. (2013). Infernal 1.1: 100-fold faster RNA homology searches. *Bioinformatics* 29, 2933–2935.
- Peters, J.E. (2019). Targeted transposition with Tn7 elements: safe sites, mobile plasmids, CRISPR/Cas and beyond. *Mol. Microbiol.* 112, 1635–1644.
- Peters, J.E., and Craig, N.L. (2001). Tn7 recognizes transposition target structures associated with DNA replication using the DNA-binding protein TnsE. *Genes Dev.* 15, 737–747.
- Peters, J.E., Makarova, K.S., Shmakov, S., and Koonin, E.V. (2017). Recruitment of CRISPR-Cas systems by Tn7-like transposons. *Proc. Natl. Acad. Sci. USA* 114, E7358–E7366.
- Price, M.N., Dehal, P.S., and Arkin, A.P. (2009). FastTree: computing large minimum evolution trees with profiles instead of a distance matrix. *Mol. Biol. Evol.* 26, 1641–1650.
- Rubin, B.E., Diamond, S., Cress, B.F., Crits-Christoph, A., He, C., Xu, M., Zhou, Z., Smock, D.C., Tang, K., Owens, T.K., et al. (2020). Targeted Genome Editing of Bacteria Within Microbial Communities. *bioRxiv*. <https://doi.org/10.1101/2019.12.11.123456v2>.
- Schmid-Burgk, J.L., Gao, L., Li, D., Gardner, Z., Strecker, J., Lash, B., and Zhang, F. (2020). Highly Parallel Profiling of Cas9 Variant Specificity. *Mol. Cell* 78, 794–800.e8.
- Steinegger, M., and Söding, J. (2017). MMseqs2 enables sensitive protein sequence searching for the analysis of massive data sets. *Nat. Biotechnol.* 35, 1026–1028.
- Strecker, J., Ladha, A., Gardner, Z., Schmid-Burgk, J.L., Makarova, K.S., Koonin, E.V., and Zhang, F. (2019). RNA-guided DNA insertion with CRISPR-associated transposases. *Science* 365, 48–53.
- Strecker, J., Ladha, A., Makarova, K.S., Koonin, E.V., and Zhang, F. (2020). Response to Comment on "RNA-guided DNA insertion with CRISPR-associated transposases". *Science* 368, eabb2920.
- Waddell, C.S., and Craig, N.L. (1988). Tn7 transposition: two transposition pathways directed by five Tn7-encoded genes. *Genes Dev.* 2, 137–149.
- Waddell, C.S., and Craig, N.L. (1989). Tn7 transposition: recognition of the attTn7 target sequence. *Proc. Natl. Acad. Sci. USA* 86, 3958–3962.

STAR★METHODS

KEY RESOURCES TABLE

REAGENT or RESOURCE	SOURCE	IDENTIFIER
<b>Bacterial strains</b>		
One Shot PIR1 Chemically Competent <i>E. coli</i>	ThermoFischer	C101010
TransformMax EC100D pir+ Electrocompetent <i>E. coli</i>	Lucigen	ECP09500
BL21(DE3) Competent <i>E. coli</i>	New England Biolabs	C2527
BL21(DE3) Electrocompetent Cells	Millipore Sigma	CMC0016
Endura ElectroCompetent Cells	Lucigen	60242
One Shot Stbl3 Chemically Competent <i>E. coli</i>	ThermoFischer	C737303
BL21-CodonPlus (DE3)-RIPL Competent Cells	Agilent	230280
<i>Trichormus variabilis</i>	ATCC	29413
<b>Chemicals, peptides, and recombinant proteins</b>		
NEBNext® High-Fidelity 2X PCR Master Mix	New England Biolabs	M0541
Q5® High-Fidelity 2X Master Mix	New England Biolabs	M0492
KAPA HiFi HotStart ReadyMix	Roche	KK2602
KOD Hot Start DNA Polymerase	Millipore Sigma	71086-3
E-Gel EX Agarose Gels, 1%	ThermoFischer	G401001
E-Gel EX Agarose Gels, 2%	ThermoFischer	G401002
E-Gel 48 Agarose Gels, 2%	ThermoFischer	G800802
Wizard® SV Gel and PCR Clean-Up System	Promega	A9282
Wizard® Genomic DNA Purification Kit	Promega	A1120
QIAquick PCR Purification Kit	QIAGEN	28106
QIAprep Spin Miniprep Kit	QIAGEN	27106
PureYield Plasmid Midiprep System	Promega	A2495
Gibson Assembly® Master Mix	New England Biolabs	E2611
NEBuilder® HiFi DNA Assembly Master Mix	New England Biolabs	E2621
Q5® Site-Directed Mutagenesis Kit	New England Biolabs	E0554
FastDigest Lglul	ThermoFischer	FD1934
Bsal-HF®v2	New England Biolabs	R3733
BbsI-HF®	New England Biolabs	R3539
T4 DNA Ligase	New England Biolabs	M0202
IPTG	Goldbio	I2481C
TRI Reagent	ZYMO RESEARCH	R2050-1-200
RNA Clean & Concentrator-25	ZYMO RESEARCH	R1017
DNase I (RNase-free)	New England Biolabs	M0303
SUPERase•In RNase Inhibitor (20 U/μL)	ThermoFischer	AM2694
Ribominus Transcriptome Isolation Kit	ThermoFischer	K155004
Terminator 5'-Phosphate-Dependent Exonuclease	Lucigen	TER51020
RiboGuard RNase Inhibitor	Lucigen	RG90910K
T4 Polynucleotide Kinase	New England Biolabs	M0201
RNA 5' Polyphosphatase	Lucigen	RP8092H
NEBNext® Small RNA Library Prep Set for Illumina® (Multiplex Compatible)	New England Biolabs	E7330
TaqMan Fast Advanced Master Mix	ThermoFischer	4444963
ddPCR Supermix for Probes (No dUTP)	Bio-Rad	#1863024
Droplet Generation Oil for Probes	Bio-Rad	#1863005
FastDigest Eco32I	ThermoFischer	FD0304

(Continued on next page)

Continued

REAGENT or RESOURCE	SOURCE	IDENTIFIER
NEBNext® Companion Module for Oxford Nanopore Technologies® Ligation Sequencing	New England Biolabs	E7180S
Flow Cell (R9.4)	Oxford Nanopore Technologies	FLO-MIN106
AMPure XP for PCR Purification	Beckman Coulter	A63881
Tn5	Schmid-Burgk et al., 2020.	N/A
cOmplete Protease Inhibitor Cocktail	Millipore sigma	4693116001
Strep-Tactin Superflow Plus	QIAGEN	30004
D-Desthiobiotin	Millipore sigma	71610-3
Ulp1 SUMO protease	F. Zhang Lab	N/A
Amicon Ultra-15 Centrifugal Filter Units 30kDa NMWL	Millipore sigma	UFC903024
Amicon Ultra-15 Centrifugal Filter Units 50kDa NMWL	Millipore sigma	UFC905024
NuPAGE 4-12% Bis-Tris Protein Gels, 1.0 mm, 12-well	ThermoFischer	NP0322BOX
NuPAGE LDS Sample Buffer (4X)	ThermoFischer	NP0007
Ampicillin, sodium salt	AmericanBio	Ab00115
Carbenicillin disodium salt, 89.0-100.5% anhydrous basis	Millipore sigma	C1389
Spectinomycin dihydrochloride pentahydrate	Millipore sigma	S4014
Kanamycin sulfate from Streptomyces kanamyceticus	Sigma	K4000
Chloramphenicol	Sigma	C0378
MiSeq Reagent Kits v2	Illumina	MS-102
NextSeq 500/550 High Output Kit v2, 75 cycles	Illumina	FC-404-2005
<b>Critical commercial assays</b>		
Qubit 1X dsDNA HS (High-Sensitivity) Assay Kit	ThermoFischer	Q33231
eStain L1 Protein Staining System	GenScript	N/A
<b>Oligonucleotides</b>		
ctgtcgtcggtagacagattaatgtcattgtgac	IDT	Insert Probe
aacgctgatgggtcacgacg	IDT	T14 LE Reverse Primer
GACTGGAGTTCAGACGTGTGCTCTTCCGATCTatctgcaaaagtctgctggg	IDT	PSP15 Target Forward Primer
GACTGGAGTTCAGACGTGTGCTCTTCCGATCTacgtactctgccacactgaag	IDT	PSP42 Target Forward Primer
cgcggaactttgtatgaccagc	IDT	<i>E. coli</i> Genome Forward Primer
ccctttcagattctgcccagcgc	IDT	<i>E. coli</i> Genome Reverse Primer
acgttcgcgtttgccgtgctgtaattgtatgac	IDT	<i>E. coli</i> Genome Probe
gagcaagagattacgagcagac	IDT	PAM library 6N upstream Primer
ctgcgtatgtggcgctgcc	IDT	PAM library 6N downstream Primer
tgaaccgaattatattgtgaacc	IDT	AvCAST RE Primer
taattgattcaacaattgtttaaccg	IDT	AvCAST LE Primer
CTTCCCTACACGACGCTCTTCCGATCTgagcaagagattacgagcagac	IDT	PAM library 6N upstream NGS Primer
CTTCCCTACACGACGCTCTTCCGATCTctgcgtatgtggcgctgcc	IDT	PAM library 6N downstream NGS Primer
GACTGGAGTTCAGACGTGTGCTCTTCCGATCTctttacttggtacaatcgtactccttagagg	IDT	AvCAST RE NGS Primer

(Continued on next page)



**Continued**

REAGENT or RESOURCE	SOURCE	IDENTIFIER
GACTGGAGTTCAGACGTGTGCTCTCCGA TCTctttatcagtaaggattcaacaattgttaaccg	IDT	AvCAST LE NGS Primer
cgacagcatcgccagtcactatg	IDT	pTarget control forward Primer for ddPCR
caagtagcgaagcgagcaggac	IDT	pTarget contro reverse Primer for ddPCR
tgcggtgatgcaatttctatgcccaccgct	IDT	pTarget control ddPCR Probe
agtcatttaataaggccactgttaaaccg	IDT	PSP1 insertion site upstream for ddPCR
ctaccgcattaaagctccgcc	IDT	PSP1 insertion site downstream Primer for ddPCR
cgacaacggcagattaatattcgaactgt	IDT	AvCAST LE ddPCR Probe
ttcgaactgtaataattgttaaccg	IDT	AvCAST-TTISS_LE 1st PCR Primer
gtctcgtggctcggagatgtgtataagagacag	IDT	TTISS 1st PCR common Primer
AATGATACGGCAGCACCCGAGATCT ACACAAGTAGAGACTCTTTCCCT ACACGACGctctccgatctTTGTTAAC CGAATCTTTGTCTAC	IDT	AvCAST-TTISS_LE 2nd PCR Primer
caagcagaagcggcctacagagatcga tcattgctcgtggctcggagatgtg	IDT	TTISS 2nd PCR comon Primer-1
caagcagaagcggcctacagagattagat cctgtctcgtggctcggagatgtg	IDT	TTISS 2nd PCR comon Primer-2
caagcagaagcggcctacagagattactgt cgtctcgtggctcggagatgtg	IDT	TTISS 2nd PCR comon Primer-3
caagcagaagcggcctacagagatggcata ggctcgtggctcggagatgtg	IDT	TTISS 2nd PCR comon Primer-4
caagcagaagcggcctacagagatcaaggc gagctcgtggctcggagatgtg	IDT	TTISS 2nd PCR comon Primer-5
caagcagaagcggcctacagagatgacgcta tgtctcgtggctcggagatgtg	IDT	TTISS 2nd PCR comon Primer-6
gcagaataaataatcctggtgctc	IDT	pTarget glmS downstream Primer for ddPCR
CTTCCCTACAGACGCTCTCCGATCT agttggcagcatcacccgacgc	IDT	pTarget glmS downstream NGS primer
tgccagatgtttgataaaaac	IDT	Non-coding region between pstS and glmS ddPCR Primer
agcgataacatgcacatcatc	IDT	glmS Primer
CTTCCCTACAGACGCTCTCCGATCT gtgattgcaccaatctctacacgctc	IDT	glmS NGS Primer
GACTGGAGTTCAGACGTGTGCTCTCCGATC Tgcaaaagttaggtccagtaacggc	IDT	PmcCAST RE NGS Primer
GACTGGAGTTCAGACGTGTGCTCTCCGATC Tgcataagcttgccgttgccg	IDT	PmcCAST LE NGS Primer
gtaagctttatatgtaaaactagaacagc	IDT	PmcCAST LE primer
CTTCCCTACAGACGCTCTCCGATCT agctccttagctcctgaaaatctcg	IDT	pTarget tRNA-Val upstream NGS Primer
tctggtactgcccagtagt	IDT	tRNA-Val primer for ddPCR
accataactttgcccgaacggcaagctta	IDT	PmcCAST LE ddPCR Probe
CACTTTCATATCAGCATACTCTGCTG	IDT	AvPSP2_Upstream Primer
CCCTCACCCAGTCACTTACTATG	IDT	AvPSP3_Upstream Primer
CTCACCCGGCAATTTCCCATTC	IDT	AvPSP4_Upstream Primer
TGTGAAGCTATGCGTTGCTGCC	IDT	AvPSP5_Upstream Primer

(Continued on next page)



**Continued**

REAGENT or RESOURCE	SOURCE	IDENTIFIER
GATTAATGTGACGGACCCGC	IDT	AvPSP6_Upstream Primer
GTCCAGTCCGATCTCTTGC	IDT	AvPSP7_Upstream Primer
CGGGCGGATCGAGTATACAC	IDT	AvPSP8_Upstream Primer
TGCCTGACTTTGCTGCGCC	IDT	AvPSP9_Upstream Primer
TATCTGATGAGTCCAAATTTAGGCC	IDT	AvPSP10_Upstream Primer
ACCGTTGCATCATGTCGCC	IDT	AvPSP11_Upstream Primer
ATTAGAAGGCGCACAAATGTTACAGC	IDT	AvPSP12_Upstream Primer
CGACAGAACACGATTGCCAGAG	IDT	AvPSP13_Upstream Primer
CTCCATTTTACCATCCAGGGC	IDT	AvPSP14_Upstream Primer
AACGCTGCAACGTCCTGAGC	IDT	AvPSP15_Upstream Primer
CAGGTGCCCGGATTACAGC	IDT	AvPSP16_Upstream Primer
CAGTGGGCATTGCGTTGC	IDT	AvPSP17_Upstream Primer
ACGTGAGCATCCTAACAGCAC	IDT	AvPSP18_Upstream Primer
TATTAGTCTGAGTATTTTTGTAGGGC	IDT	AvPSP19_Upstream Primer
GGACGTTAAAACGTCACGGCC	IDT	AvPSP20_Upstream Primer
GTCTGTGCGCTATGCTATATTGG	IDT	AvPSP21_Upstream Primer
GAATTCGCTTTCTTGAGAGCTTCTG	IDT	AvPSP22_Upstream Primer
ATCTGAGGCTTTGCACTCTGC	IDT	AvPSP23_Upstream Primer
TGAGTCGCCCGGAACCTCG	IDT	AvPSP24_Upstream Primer
GCTTAAGAATCGTAGAACCATCGGC	IDT	AvPSP25_Upstream Primer
GAGCCCGTGAACGAACTC	IDT	AvPSP26_Upstream Primer
CGACGGTGGTACGCATAACTTTC	IDT	AvPSP27_Upstream Primer
CGGTTTTACCCCTGTTACACGGG	IDT	AvPSP28_Upstream Primer
CTGCTAAAAATCGGCGCTAAGAACC	IDT	AvPSP29_Upstream Primer
CAGCTGAGACTGAGTTTTTCCAGC	IDT	AvPSP30_Upstream Primer
CTGTGCGGTGCCACAATCGG	IDT	AvPSP31_Upstream Primer
GCTGTTAGTCATGATTGCCTGC	IDT	AvPSP32_Upstream Primer
CATCCGGCATTAAAGCACCAACC	IDT	AvPSP33_Upstream Primer
GAAATGAACGATTATCCCTATCAAGC	IDT	AvPSP34_Upstream Primer
CAACCAGGCAACATGCCCGAC	IDT	AvPSP35_Upstream Primer
TGGCTATTCATTGAAAGGAGGCTCG	IDT	AvPSP36_Upstream Primer
GTCATTCGCTGCATATCATGAACGC	IDT	AvPSP37_Upstream Primer
TTGCATTCTGCGGGAAGGATATC	IDT	AvPSP2_Downstream Primer
AGCGAATAGACAAATCGGTTGCCG	IDT	AvPSP3_Downstream Primer
GCCTGTGAACACACAGACAGAG	IDT	AvPSP4_Downstream Primer
GACTCTAACCGTCGGCCCC	IDT	AvPSP5_Downstream Primer
CTCATCGCCATTACCTTCATGATAG	IDT	AvPSP6_Downstream Primer
GATCTGCGTTTTACAACCTCAGATCAC	IDT	AvPSP7_Downstream Primer
CGGAAATCATACCATGAGGTTAATCC	IDT	AvPSP8_Downstream Primer
TGAACATAACGCGATAGCAAAGG	IDT	AvPSP9_Downstream Primer
TGGGCAAATCAAGATACGCGCAG	IDT	AvPSP10_Downstream Primer
TAATTGCTAAGGAATAACCCAGTTGC	IDT	AvPSP11_Downstream Primer
CCTGGCCGTAATGAAACACGC	IDT	AvPSP12_Downstream Primer
CTGAAAAAGTTGTCCGCGATGC	IDT	AvPSP13_Downstream Primer
GCGCGGGGAACACTCTAAAC	IDT	AvPSP14_Downstream Primer
CGTAAGTTTCGACGCTTATTAACAGC	IDT	AvPSP15_Downstream Primer
CCTTATCCGCGCTACAAAGTCCG	IDT	AvPSP16_Downstream Primer
TTCTACGGGCAGGATGACTGG	IDT	AvPSP17_Downstream Primer

(Continued on next page)

**Continued**

REAGENT or RESOURCE	SOURCE	IDENTIFIER
CGTGGGAAGGAGGCTAATGG	IDT	AvPSP18_Downstream Primer
GCGTTCTGGTTGAATGGAACGC	IDT	AvPSP19_Downstream Primer
GTTGCCAGCAGGTATTATATCGCC	IDT	AvPSP20_Downstream Primer
GCAATGTTGCACCGTTTGCTGC	IDT	AvPSP21_Downstream Primer
GGTGGTTGACCTAAGGTAGCAG	IDT	AvPSP22_Downstream Primer
CCTTTCGCCCTGAATGCAGTC	IDT	AvPSP23_Downstream Primer
TCCGACAGTAAGCAAAAATTTGAGAC	IDT	AvPSP24_Downstream Primer
AGGTATTTAACCTGTGTTGATTGCTG	IDT	AvPSP25_Downstream Primer
ACGCAGCATTAAATGCATAGTGGTTAAG	IDT	AvPSP26_Downstream Primer
GCGGGGCATTTTCTCCTGTTATG	IDT	AvPSP27_Downstream Primer
CACTAAACCGGGCCGTTTAGCC	IDT	AvPSP28_Downstream Primer
CATATTGCGCATGTTGCGGCAC	IDT	AvPSP29_Downstream Primer
GAAAAGCGCGCAAAGTGCGG	IDT	AvPSP30_Downstream Primer
GAATGCTTACTGAAGACCGCGC	IDT	AvPSP31_Downstream Primer
CAAGAACAAGGCCATCCCTTTACC	IDT	AvPSP32_Downstream Primer
CCACTGTGTCGCTAAAAGAGACAAAC	IDT	AvPSP33_Downstream Primer
TTTGAGCCTGGCTTATCGCCG	IDT	AvPSP34_Downstream Primer
ATGATGCGGGTTCGATTCGCCG	IDT	AvPSP35_Downstream Primer
CCGCCAGCTGAAGAAATCGCTAATTC	IDT	AvPSP36_Downstream Primer
CATCGGCTACGATGAAAAATGGGTC	IDT	AvPSP37_Downstream Primer
<b>Recombinant DNA</b>		
pHelper_ShCAST	Addgene	#127922
pUC19 Vector	New England Biolabs	N3041
pBluescript II SK (+)	Agilent	212205
pCDFDuet-1 DNA	Millipore sigma	71340
pCOLADuet-1 DNA	Millipore sigma	71406
pDonor(pSC101 origin)_ShCAST	F. Zhang Lab	N/A
pACYC 6N PAM library	<a href="#">Strecker et al., 2019</a>	N/A
pDonor_ShCAST_kanR	Addgene	#127924
<b>Software and algorithms</b>		
Geneious	<a href="https://www.geneious.com/">https://www.geneious.com/</a>	v2020
QuantaSoft Software	Bio-Rad	#1864011
Hmmer	<a href="http://hmmer.org/">http://hmmer.org/</a>	v3.1
Blast+	<a href="http://blast.ncbi.nlm.nih.gov//blast.ncbi.nlm.nih.gov/Blast.cgi">http://blast.ncbi.nlm.nih.gov//blast.ncbi.nlm.nih.gov/Blast.cgi</a>	v2.9.0
iTOL	<a href="https://itol.embl.de/">https://itol.embl.de/</a>	N/A
MAFFT	<a href="https://mafft.cbrc.jp/">https://mafft.cbrc.jp/</a>	V7.407
Minced	<a href="https://github.com/ctSkennerton/minced">https://github.com/ctSkennerton/minced</a>	v0.4.2
Prodigal	<a href="https://github.com/hyattpd/Prodigal">https://github.com/hyattpd/Prodigal</a>	v2.6.3
tRNA-ScanSE	<a href="http://lowelab.ucsc.edu/tRNAscan-SE/">http://lowelab.ucsc.edu/tRNAscan-SE/</a>	v2
Infernal	<a href="http://eddylab.org/infernal/">http://eddylab.org/infernal/</a>	v1.1.3
PyMOL	<a href="https://pymol.org/2/">https://pymol.org/2/</a>	v1.2
FastTree	<a href="http://www.microbesonline.org/fastree/">http://www.microbesonline.org/fastree/</a>	v2.1
Hydrophobic Cluster Analysis	<a href="http://osbornite.impmc.upmc.fr/hca/hca-form.html">http://osbornite.impmc.upmc.fr/hca/hca-form.html</a>	N/A
<b>Other</b>		
Bench Protocol	(this paper)	STAR Methods



## RESOURCE AVAILABILITY

### Lead contact

Further information and requests for resources should be directed to and will be fulfilled by the Lead Contact, Feng Zhang ([zhang@broadinstitute.org](mailto:zhang@broadinstitute.org)).

### Materials availability

Plasmids generated in this study have been deposited to Addgene.

### Data and code availability

Expression plasmids are available from Addgene under a uniform biological material transfer agreement; support forums and computational tools are available via the Zhang lab website (<https://zlab.bio/>). All CAST loci are available in [Data S1](#) as an archive of GenBank files.

## EXPERIMENTAL MODEL AND SUBJECT DETAILS

### Bacteria strains

For transposition assays, *E. coli* strains were plated on LB-agar plates supplemented with appropriate antibiotics and IPTG and incubated at 37°C for 17 hours. For recovery of mature crRNAs and Tns proteins of I-B CAST systems, *E. coli* from a single colony were grown in Terrific Broth media (TB) at 37°C until OD600 reached 0.6, and further grown at 16°C with IPTG supplementation for expression. Culture for *Trichormus variabilis* followed the condition suggested by ATCC. *Scytonema holmanni* (UTEX B 2349) and *Anabaena cylindrica* (PCC 7122) were cultured in BG-11 media at 25°C with light periodicity of 14 hours on, 10 hours off.

## METHOD DETAILS

### Plasmid construction

All plasmids used in this study are described in [Table S2](#). For ShCAST homing analysis, a tRNA target plasmid was cloned in the pACYC background by rejoining the chromosomal sequence up and downstream of the transposon. ShCAST pHelper plasmids (Addgene #127922) with endogenously driven tracrRNA were modified by replacing the previous FnPSP1 spacer with various crRNA driven by the J23117 promoter and flanked with the T7Te terminator using Gibson Assembly (NEB). The 24-nt 5' extension and 14-nt 3' extensions of the delocalized crRNA were taken from the natural host to match the length of crRNA derived from the CRISPR array. For sgRNA experiments targeting the *E. coli* genome, the pHelper\_ShCAST\_sgRNA plasmid (Addgene #127922) was modified by cloning spacers using Golden Gate assembly and Lgal. For all RNA truncations, the length of crRNA or sgRNA spacer was reduced, and mismatches were generated with transversion mutations (A to T, T to A, G to C, C to G). All tested crRNA and sgRNA can be found in [Table S2](#). For AvCAST experiments, genes encoding TnsA-TnsB-TnsC-TniQ, TnsD and Cas6-Cas8-Cas7-Cas5 were amplified from the genome of *Trichormus variabilis* (*Anabaena variabilis* ATCC 29413). All the Tns genes were cloned into pCOLADuet-1 (Millipore) and the Cascade genes were cloned into pCDFDuet-1 (Millipore), resulting in pTns(AvCAST) and pCascade(AvCAST)\_ΔCRISPR, respectively using Gibson Assembly Master Mix (NEB). A pCascade was generated by inserting a tandem BsaI site flanked by two CRISPR direct repeats into pCascade(AvCAST)\_ΔCRISPR, and specific guides were further inserted by BsaI digestion and ligation. The Tns expression cassette in pTns(AvCAST) was inserted into pCascade(AvCAST) to obtain pHelper(AvCAST). For PmcCAST experiments, genes encoding '*Peltigera membranacea cyanobiont*' 210A TnsAB-TnsC-TnsD, TniQ, and Cas6-Cas8-Cas7-Cas5 were synthesized (Twist Bioscience) and cloned into pCDFDuet-1 with the appropriate spacer flanked by two CRISPR direct repeats described above. Gene fragments encoding both transposon ends (GENEWIZ) were cloned into pBluescript II SK (+), yielding pDonor(AvCAST) or pDonor(PmcCAST). For PAM screens, a 0.5kb exon fragment amplified from human *EMX1* was inserted between the transposon ends as a mock non-functional cargo in *E. coli*. For other experiments, a chloramphenicol resistance gene (CmR) was used as cargo. To obtain pTns variants, the Q5 Site-Directed Mutagenesis Kit (NEB) was used. For Nanopore sequencing experiments, all CAST components (DR-spacer-DR, Cascade, and Tns proteins) were cloned under a constitutive lac promoter to obtain pHelper2(AvCAST) and pHelper2(PmcCAST). The design of pR6K donors for AvCAST and PmcCAST followed that of pDonor\_ShCAST\_kanR (Addgene #127924). The *gImS* locus of BL21(DE3) (3800227-3801226, CP001509) was cloned into pUC19 (NEB). The *gImS* gene of *A. variabilis* and tRNA-Val gene of '*Peltigera membranacea cyanobiont*' 210A were cloned into pACYC vector bearing AvPSP1 or PmcPSP1 flanked by an AT or ATG PAM, respectively. These target plasmids were used as pTarget for *in vitro* transposition assays and also pTarget for assays in bacteria.

### PAM and insert position analysis of AvCAST and PmcCAST

To identify the PAM of AvCAST and PmcCAST, 100 ng of randomized 6N sequence-containing pACYC vector libraries ([Strecker et al., 2019](#)) was co-electroporated with 100 ng of both pHelper and pDonor into BL21(DE3) electrocompetent cells (Sigma). Cells were recovered for 1 hour and plated on 100 μg/ml carbenicillin, 50 μg/ml spectinomycin, and 50 μg/ml chloramphenicol containing LB-agar plates. After 37°C incubation for 17 hours, all colonies were scraped from the plates, and a portion was re-plated on 0.1 mM

IPTG supplemented triple antibiotic LB-agar plates to induce protein expression. Cells were incubated for an additional 17 hours at 37°C. All colonies were scraped and plasmid DNAs were prepared from the colonies using the PureYield Plasmid Midiprep System (Promega). Insertion products containing the 6N sequence were amplified and sequenced using a MiSeq Reagent Kit v2, 300-cycle (Illumina). PAM and insert position were characterized using an established pipeline (Strecker et al., 2019).

#### ***E. coli* Transposition Assays**

For ShCAST, transposition in *E. coli* was performed by transformation of 20 ng each of pHelper, pTarget, and pDonor into Transform Max EC100 pir+ Electrocompetent *E. coli* (Lucigen). Cells were recovered for 1 hour and plated on ampicillin, kanamycin, and chloramphenicol-containing plates. Cells were harvested 20 hours after plating, and scraped cells were lysed in 15  $\mu$ L colony lysis buffer (TE with 0.1% Triton X-100). Genome targeting experiments were performed in a similar manner using pHelper and pDonor plasmids followed by plating on ampicillin and kanamycin. Cells were boiled for 5 min, diluted with 60  $\mu$ L of water, spun at 4000  $\times$  g for 10 min to pellet debris, and the supernatant was used for subsequent analysis. The frequency of genome insertions relative to the concentration of extracted *E. coli* genomes or to the target plasmid was determined with qPCR as described above with a guide-specific forward primer and a primer/probe set in an unmodified region of the *E. coli* genome or the pTarget chloramphenicol resistance gene (Table S2). The initial homing test for ShCAST was performed with a modified pHelper plasmid harboring a deletion of *cas12k*.

For AvCAST, 10 guides with 5' AT PAMs were chosen in non-coding regions of the *E. coli* genome (Strecker et al., 2019) and cloned into pCascade(AvCAST) (Table S2). Each 100 ng of pCascade(AvCAST) targeting a specific genomic region was co-electroporated with pTns(AvCAST) $\Delta$ TnsD and pDonor(AvCAST) into BL21(DE3) electrocompetent cells (Sigma) and plated on 100  $\mu$ g/ml carbenicillin, 50  $\mu$ g/ml spectinomycin, and 50  $\mu$ g/ml kanamycin containing LB-agar plates. After 37°C incubation for 17 hours, all colonies were scraped from the plates, and a portion was re-plated on 0.1 mM IPTG supplemented triple antibiotic LB-agar plates to induce protein expression. Cells were incubated for an additional 17 hours at 37°C. All colonies were scraped and the gDNA was purified using the Wizard Genomic DNA Purification Kit (Promega). Insertions were identified by PCR using KAPA HiFi HotStart ReadyMix (Roche). The frequency of genome insertions was determined with droplet digital PCR (ddPCR) as described below with 20 ng template gDNA for 20  $\mu$ L ddPCR reaction.

#### **Nanopore sequencing to determine constitutive/replicative transposition**

Transposition assays for AvCAST and PmcCAST were performed by transformation of 30 ng each of pHelper2, pR6K Donor, and pTarget(AT/ATG+AvPSP1/PmcPSP1) into Pir1 *E. coli*. Cells were recovered for 1 hour at 37°C and plated on 50  $\mu$ g/ml kanamycin, 50  $\mu$ g/ml spectinomycin, and 50  $\mu$ g/ml chloramphenicol containing LB-agar plates. Cells were harvested 5 days after incubation at room temperature, and subjected to mini-prep by QIAprep Spin Miniprep Kit (QIAGEN). Note that we avoided incubation at 37°C to prevent transposed products being actively resolved, which would mask replicative transposition. To recover transposed products, 100 ng mini-prep product was electroporated into Endura Competent Cells (Lucigen). Cells were recovered for 1 hour and plated on 50  $\mu$ g/ml kanamycin and 50  $\mu$ g/ml chloramphenicol containing LB-agar plates, and further incubated at room temperature for 5 days. Donor insertion on pTarget was confirmed by Sanger sequencing (position and target site duplication) of mini-prep products for 12 colonies. In parallel, all colonies were harvested and subjected to mini-prep, followed by amplification-free Nanopore sequencing library preparation (Oxford Nanopore Technologies SQK-LSK109). Briefly, mini-prep products were linearized by EcoRV, followed by end-prep and subsequent ligation of sequencing adapters. Resulting libraries were loaded on a MinION R9 flow cell and sequenced. Sequence reads containing 20 bp of AvPSP1/PmcPSP1 and both 20 bp of the outer transposon LE and RE were filtered for further analysis, thereby discarding short, low-quality, and contaminating gDNA reads.

#### **Droplet digital PCR (ddPCR) reactions**

Insertion events were quantified using insertion specific primers and a donor specific probe (Table S2). ddPCR Supermix for Probes (No dUTP) (BioRad), primers (900 nM each), a probe (250 nM), and template DNA were combined into 20  $\mu$ L reactions, and droplets were generated with 70  $\mu$ L of Droplet Generation Oil for Probes (BioRad) using the QX200 Droplet Generator (BioRad). Thermal cycling conditions for ddPCR reactions were as follows: 1 cycle, 95°C, 10 min; 40 cycles, 94°C, 30 s, 58°C, 1 min; 1 cycle, 98°C, 10 min; 4°C hold. PCR products were read with a QX200 Droplet Reader, and absolute concentrations of inserts were determined using QuantaSoft (v1.6.6.0320). Total template (genome or target plasmid) amount was also quantified through this process, and insertion frequency was calculated as inserts/template.

#### **TTISS for AvCAST insertion specificity analysis**

AvPSP2, 7, and 12 sites on the *E. coli* genome were targeted as mentioned above, with the following change: 100 ng of a temperature-sensitive pSC101-donor was used. After incubation on IPTG supplemented triple antibiotic LB-agar plates, cells were re-plated and grown for 12 hours at 43°C to prevent unintended amplification of donor plasmids in the following Tagmentation-based Tag Integration Site Sequencing (TTISS) analysis (Schmid-Burgk et al., 2020). Genomic DNA was extracted from hundreds of colonies on a LB-agar Petri dish, and 500 ng genomic DNA (from approximate  $10^9$  *E. coli* cells) was tagmented with Tn5, and re-purified by Wizard SV Gel and PCR Clean-Up System (Promega). Tagmented DNA samples were amplified using two rounds of PCR with KOD Hot Start DNA Polymerase (Millipore) using a Tn5 adaptor-specific primer and nested primers within the DNA donor (Table S2). The resulting libraries were sequenced using a NextSeq v2 kit, 75 cycle kit with 45 forward cycles and 30 reverse cycles. Read pairs with R1

containing the terminal 27 bp of the transposon RE sequence were filtered for further analysis and trimmed of the transposon sequence for alignment to the *E. coli* genome (CP001509). Filtered and trimmed reads were imported into Geneious Prime and aligned using the Geneious aligner with medium-low sensitivity, no fine-tuning, no structural variant, insertion, or deletion discovery enabled, and requiring paired reads to map nearby. The resulting SAM files were exported for further analysis. Aligned R1 reads with length of 18 bp (remaining R1 length after trimming of 27 bp of transposon sequence) and SAM flags 99 (insertion position = POS field) or 147 (insertion position = POS field + trimmed R1 length of 18 bp) were used to determine the transposon insertion position. Reads with an insertion position 50-100-bp downstream of the PAM were considered on-target, whereas remaining reads were counted as off-targets.

#### qPCR Reactions

Quantitative PCR reactions were performed using TaqMan Fast Advanced Master Mix (Applied Biosystems) using 20  $\mu$ L reactions, 2  $\mu$ L input of extracted nucleic acid, 900 nM forward primer, 900 nM reverse primer, and 250 nM of probe. Reactions were quantified using the LightCycler 480 Instrument (Roche).

#### RNA sequencing to recover mature crRNAs

To recover mature RNAs of AvCAST and PmcCAST, each pCascade(AvCAST, AvPSP1 spacer) and pCascade(PmcCAST, PmcPSP1 spacer) was transformed into BL21-CodonPlus (DE3)-RIPL Competent Cells (Agilent 230280). A 10-mL culture was grown in Terrific Broth media (TB) supplemented with 50  $\mu$ g/ml spectinomycin at 37°C with shaking at 150 rpm until an OD600 of 0.6 was reached. Cascade and crRNA expression was induced by supplementation with IPTG to a final concentration of 0.5 mM. The cells were incubated at 16°C for 16 h, and then harvested by centrifugation for 10 min at 4°C at 4000 rpm. Total RNA was extracted by TRIzol-chloroform (ZYMO RESEARCH) and DNaseI treatment. Ribosomal RNAs were removed by Ribominus Transcriptome Isolation Kit (Invitrogen), and the remaining RNA was treated with 5' terminator exonuclease, T4 Polynucleotide Kinase, RNA 5' polyphosphatase, and used as input for NEBNext Small RNA Library Prep Set for Illumina (NEB). Prepared libraries were sequenced using a NextSeq 500/550 High Output Kit v2, 75 cycles. Paired-end reads were aligned to their respective reference expression plasmid sequences using BWA. Resulting transcript sequences were analyzed using Geneious Prime.

#### Purification of Tn7-like machinery components and *in vitro* transposition assays

TnsA, B, C, and D of AvCAST and TnsAB, C, and D of PmcCAST were individually cloned into ColE1-based pTwinStrep-SUMO bacterial expression vectors. Each vector was transformed into BL21-CodonPlus (DE3)-RIPL Competent Cells. A 5-mL starter culture was grown in TB supplemented with 100  $\mu$ g/ml ampicillin for 12 h, which was used to inoculate 4 L of TB for growth at 37°C with shaking at 150 rpm until an OD600 of 0.6 was reached. Protein expression was induced by supplementation with IPTG to a final concentration of 0.5 mM. The cells were incubated at 16°C for 16 h for protein expression, and then harvested by centrifugation for 20 min at 4°C at 4000 rpm (Beckman Coulter Avanti J-E, rotor JLA9.100). Cell pellets were stored at -80°C for later purification. All subsequent steps were performed at 4°C. Cell pellets were resuspended in 200 mL of lysis buffer (50 mM Tris-HCl, 500 mM NaCl, 10% glycerol, 1 mM DTT, pH 8.0) supplemented with cComplete Protease Inhibitor Cocktail (Millipore Sigma 4693116001). Cells were disrupted using the LM20 Microfluidizer system at 18,000 PSI. Lysate was cleared by centrifugation for 30 min at 4°C at 9500 rpm (Beckman Coulter Avanti J-E, rotor JLA-10.500). The cleared lysate was applied to 2 mL of packed Strep-Tactin Superflow Plus (QIAGEN 30004) and incubated with rotation for 1 h, followed by washing of the protein-bound beads in 50 mL of lysis buffer. The bound SUMO-tagged proteins were eluted in 10 mL of lysis buffer supplemented with 2.5 mM desthiobiotin (Sigma). The eluted proteins were further digested by Ulp1 SUMO protease at 4°C for 16 h. Resulting Tns proteins were concentrated using Amicon Ultra Centrifugal Filter Units (Millipore), and protein concentration was estimated by NuPAGE (Invitrogen) and eStain L1 Protein Staining System (GenScript). The concentrated protein was loaded onto a gel filtration column (Superdex 200 Increase 10/300 GL, GE Healthcare) equilibrated with storage buffer (50 mM Tris-HCl, 500 mM NaCl, 5% glycerol, 2 mM DTT, pH 7.5) via FPLC. The resulting fractions from gel filtration were analyzed, and the fractions containing the protein were pooled, snap frozen as 1 mg/mL aliquots, and stored at -80°C. *In vitro* transposition reactions were carried out with 200 nM of each Tns protein, 100 ng of pDonor(AvCAST)\_CmR, and 100 ng of pTarget for AvCAST *in vitro* (*E. coli* - glms) in a final reaction buffer of 26 mM HEPES pH 7.5, 5 mM Tris-HCl pH 8.0, 50  $\mu$ g/mL BSA, 2 mM ATP, 2.1 mM DTT, 0.05 mM EDTA, 0.2 mM MgCl<sub>2</sub>, 50 mM NaCl, 21 mM KCl, 1% glycerol supplemented with 15 mM Mg(OAc)<sub>2</sub> based on *in vitro* Tn7 reaction protocol (Bainton et al., 1991). Total reaction volumes were 20  $\mu$ L, and reactions were incubated for 2 hours at 30°C. For PmcCAST, pDonor(PmcCAST)\_CmR and pTarget for PmcCAST (bearing ATG+PmcPSP1 and trnA-Val) were used. The resulting products were purified using Wizard SV Gel and PCR Clean-Up System (Promega), followed by diagnostic PCR.

#### Comparative genomic analysis of CAST loci and TniQ/TnsD analysis

We searched for new CAST loci using type I-F, I-B, and V-K components in prokaryotic and metagenomic databases (nucleotide sequence available in August 2019 in NCBI database restricted to Prokaryotic sequences WGS and GenBank, and MG-RAST) (Keegan et al., 2016). First, we identified contigs where CAST components (TnsA, TnsB, TnsC, TniQ/TnsD plus Cascade IB, and TnsB, TnsC, TniQ plus Cas12k) are colocalized to form a full CAST locus (CAST-IB: TnsA, TnsB, TnsC, TniQ/TnsD plus Cascade IB; CAST-IV: TnsB, TnsC, TniQ plus Cas12k) within a 50-kb region using tblastn (bitscore superior or equal to 30) (Altschul et al.,



1990) from each CAST component extracted from previous literature (Faure et al., 2019a; Peters et al., 2017). Then, we extracted each CAST component from all contigs, clustered them by protein type (TnsA, TnsB, TnsC, TniQ/TnsD, Cas6Ib, Cas7b, Cas8b, Cas5b, Cas12k) and by sequence similarity using mmseqs2 (Steinegger and Söding, 2017) (50 percent of sequences identity 50 percent of coverage), aligned members together within each clusters using mafft-einsi (Kato et al., 2005), and created a hmm profile for each cluster using hmmer (Eddy, 2009; Kato et al., 2005). From these profiles, we searched for additional contigs where CAST components (TnsA, TnsB, TnsC, TniQ/TnsD plus Cascade IB, and TnsB, TnsC, TniQ plus Cas12k) are colocalized within a 50-kb region using hmmsearch (bitscore superior or equal to 30) against a translated version of our nucleotide database. For each CAST locus, we predicted gene boundaries using prodigal version 2.6.3 (model meta) (Hyatt et al., 2010) and Cas profiles database (Makarova et al., 2020). We predicted CRISPR arrays using minced software (<https://github.com/ctSkennerton/minced>) (minimum repeat size 16, maximum repeat size 50, minimum spacer size 20, maximum spacer size 50). We predicted tRNA and other ncRNA using tRNA-ScanSE version 2 (Chan and Lowe, 2019) and Infernal version 1.1.3 (Chan and Lowe, 2019; Griffiths-Jones et al., 2003; Nawrocki and Eddy, 2013) with Rfam database. Transposon ends were determined manually on Geneious framework (Kearse et al., 2012; Price et al., 2009) using the following methodology. We searched for repeat segments of 10 nucleotides with a maximum of 3 mismatched nucleotides and looked for inverted repeats embedding both the transposon components and the Cas components. For every candidate, we used the opposite inverted repeat and ran a similar search. We looked for two blocks of inverted clustered repeats that embed CAST components and validated the ends when possible by searching for the duplication site on both sides of the transposon. If no candidate was found with this repeat search method, we used blastn-short (Altschul et al., 1990) (word size = 7) to initially identify repeats, and performed the same downstream strategy to find the transposon's ends. The structural comparison of TniQ was performed under PyMOL framework version 1.2 (The PyMOL Molecular Graphics System, Schrödinger, LLC) and using Hydrophobic Cluster Analysis (Callebaut et al., 1997; Faure and Callebaut, 2013a, 2013b). Phylogenetic trees were built with FastTree (Price et al., 2009) using the Whelan And Goldman model (WAG model) and visualized with iTOL (Letunic and Bork, 2007).

#### QUANTIFICATION AND STATISTICAL ANALYSIS

The number and definition of replicates for each experiment can be found in the corresponding figure legend. To quantitatively define PAM preference, insertion read counts stratified by the PAM sequence at the 6N randomized library position were normalized by abundance of the corresponding PAM in the input library. PAMs displaying greater than 16-fold enrichment in abundance compared to the input library were input into WebLogo (<https://weblogo.berkeley.edu/>) to obtain the corresponding sequence logo. Sequencing data was converted to coverage maps using Geneious Prime and its built-in Geneious aligner. All remaining quantitative data was processed and visualized using GraphPad Prism.

Supplemental figures

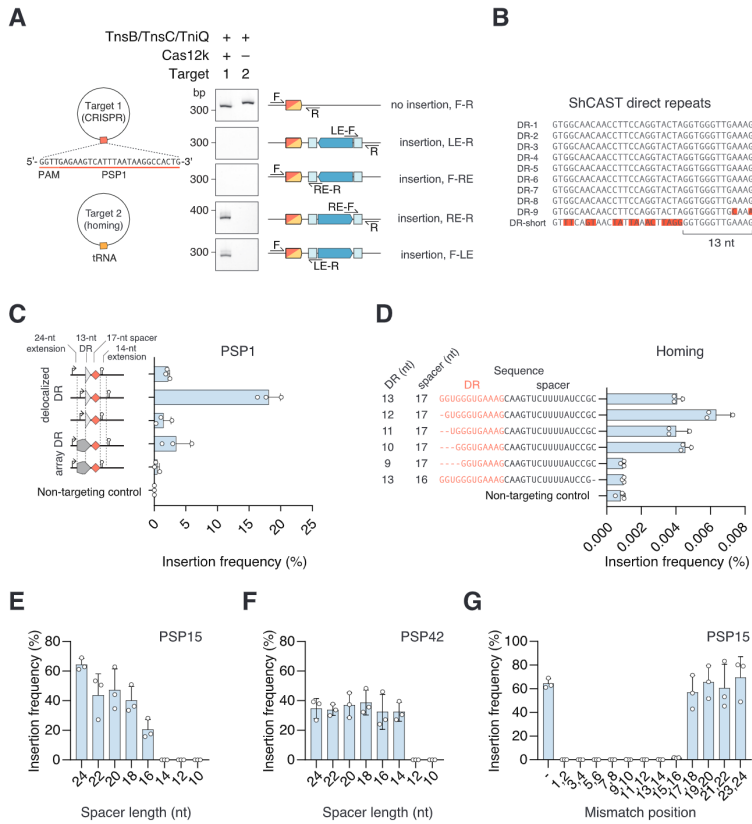


**Figure S1. Characterization of type V-K CAST short, delocalized crRNA, related to Figure 1**

(A) Insertion activity of ShCAST components in *E. coli* into a CRISPR and homing target plasmid. (B) Alignment of typical direct repeats from the CRISPR array with short direct repeat from ShCAST. (C) Insertion activity of crRNA containing the delocalized direct repeat or the array direct repeat with a PSP1 spacer; promoters and terminators are indicated with an arrow and hairpin, respectively. Both the 17-nt spacer and 14-nt spacer extension match the target sequence. Data are represented as mean  $\pm$  SD (D) Insertion activity of ShCAST homing following truncation of its delocalized crRNA. Data are represented as mean  $\pm$  SD (E) Effect of sgRNA spacer length on insertion frequency of ShCAST on PSP15 through deletion of 3' spacer sequence. Data are represented as mean  $\pm$  SD (F) Effect of sgRNA spacer length on insertion frequency of ShCAST on PSP42 through deletion of 3' spacer sequence. Data are represented as mean  $\pm$  SD (G) Effect of double mismatches in the sgRNA spacer at the indicated positions on insertion frequency of ShCAST on PSP15. Positions are relative to the 5' NGTN PAM. Data are represented as mean  $\pm$  SD.

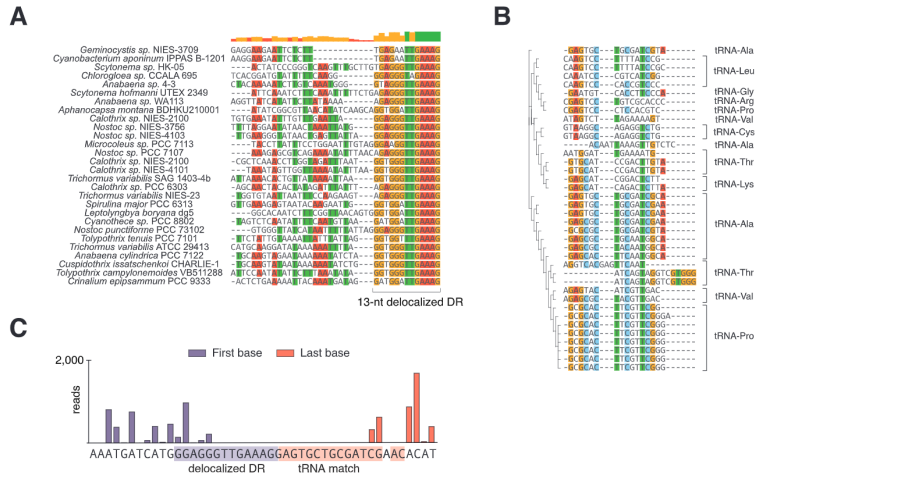


**Figure S2. Comparison of delocalized crRNA across type V-K CAST systems, related to Figure 2**  
 (A) Alignment of delocalized direct repeats from diverse type V-K CAST systems. (B) Alignment of spacers from delocalized crRNA of type V-K CAST systems, annotated with their corresponding tRNA target. (C) Start and end position of RNA sequencing reads aligned to the predicted delocalized crRNA in *A. cylindrica*. The predicted delocalized DR and tRNA match are annotated as determined by homology to the canonical DR and downstream tRNA target respectively.

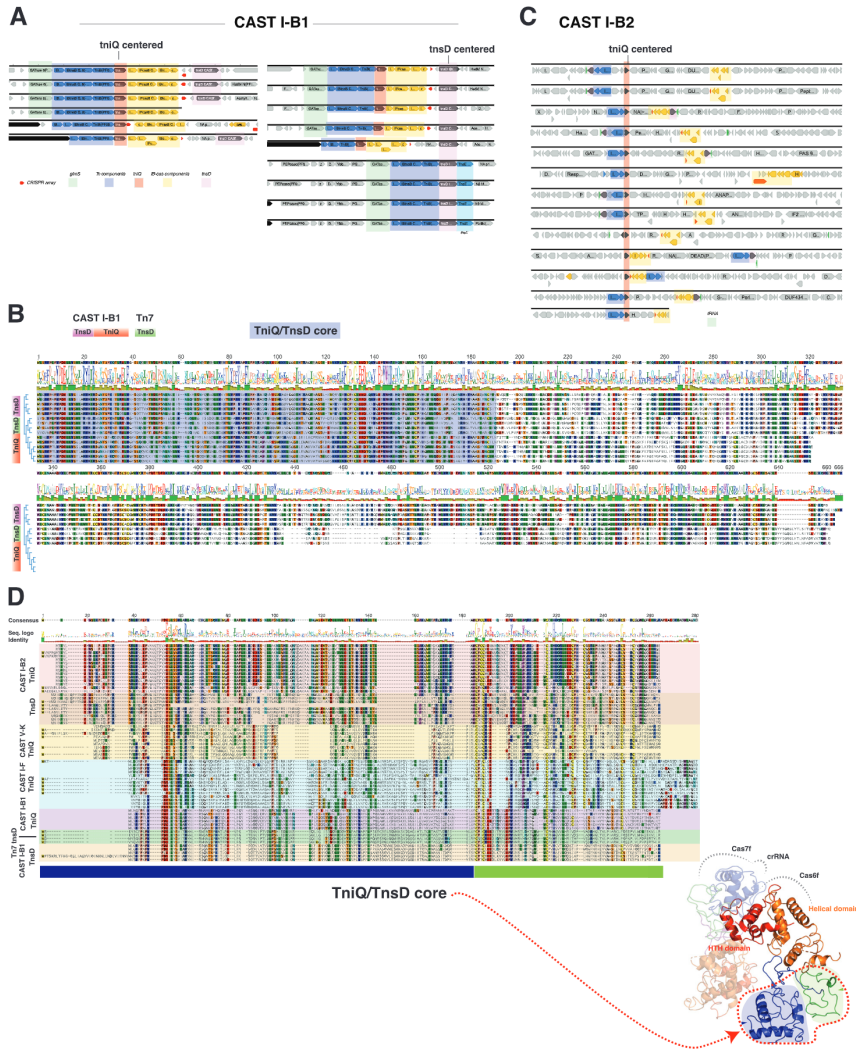
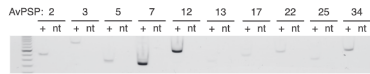


**Figure S3. CAST I-B loci comparison and TnsD/TniQ analysis, related to Figures 3 and 6**  
 (A) Left, CAST I-B1 loci sharing similar TniQ (non identical and greater than or equal to 50 percent sequence identity). Right, Loci sharing similar CAST I-B1 *tnsD* (greater than or equal to 50 percent sequence identity). *tniQ* is colored in red, transposon core genes (*tnsA*, *tnsB*, and *tnsC*) in blue, Cas components in yellow, (legend continued on next page)

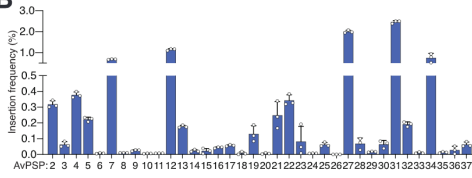
*glmS* homing gene in green, CRISPR arrays are shown as thin empty red arrays, and *tnsD* in pink. Black arrows represent padding to center the *tniQ* or *tnsD* genes. Cyan indicates *tnsE*, a hallmark gene for targeting conjugative plasmids in Tn7. Loci centered on *tnsD* (right) include Tn7 loci (non CAST) that also home to *glmS* (green). All loci are available in the Supplemental Dataset (B) Protein sequence alignment of CAST I-B1 TniQ (red), TnsD (purple), and Tn7-TnsD (green) sharing sequence similarity with CAST I-B1 TnsD. Sequences are ordered from a tree built with FastTree (WAG model) (Price et al., 2009). Blue highlights indicate the conserved core of TniQ/TnsD. On top of the alignment sequences are the consensus, the hydrophobicity graph (red), and the conservation graph (green). The alignment is colored using the Rasmol color palette; colored positions indicate conservation in agreement with the consensus sequence. Tn7 TnsD and CAST-IB TnsD are longer than TniQ, and are similar in their C-terminal region. (C) CAST I-B2 loci sharing similar TniQ (non identical and greater than or equal to 50 percent sequence identity). *tniQ* is colored in red, transposon core genes (*tnsAB* and *tnsC*) in blue, Cas components in yellow, tRNA homing gene in green, CRISPR arrays are shown as thin empty red arrays, and *tnsD* in pink. (D) Protein alignment of TniQ/TnsD core region from CAST I-B TniQ (red), TnsD (purple), and Tn7-TnsD (green), CAST I-F TniQ (light green), and CAST V-K TniQ (orange). On top of the alignment sequences are the consensus and the conservation graph (green). The alignment is colored using the Rasmol color palette; colored positions indicate conservation in agreement with the consensus sequence. Domain annotation of TniQ dimer mapped on the electron microscopy structure (PDB: 6pij) (Halpin-Healy et al., 2020) of CAST I-F TniQ. The different colors indicate the potential domains of TniQ, from N-terminal to C-terminal, blue, green, orange, and red. TniQ/TnsD core (red dashed line) is formed by the blue and the green domain (region conserved in CAST TniQ/TnsD and Tn7-TnsD). Black dashed lines indicate interaction with Cascade components found in the structure.



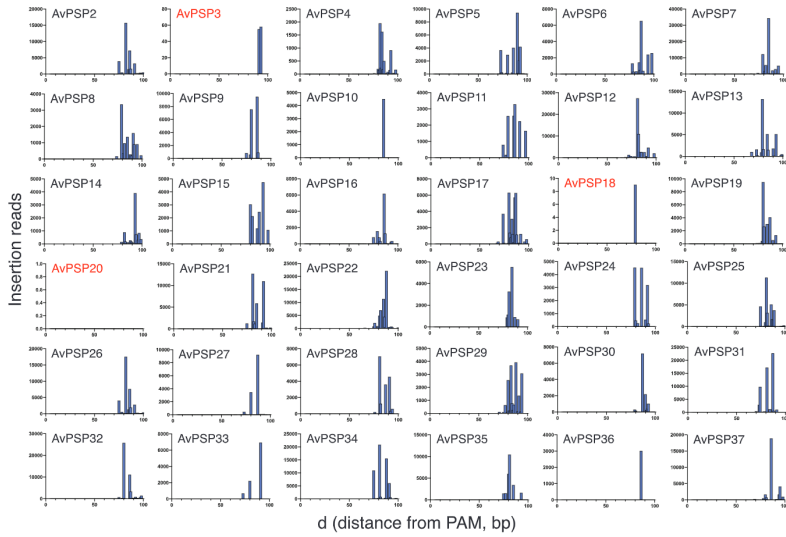
**A**



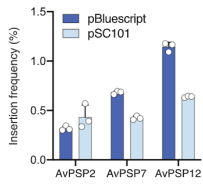
**B**



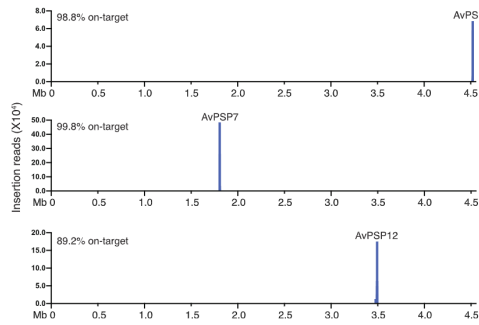
**C**



**D**



**E**



(legend on next page)



---

**Figure S4. RNA-guided transposition on *E.coli* genome by type I-B subtype1 AvCAST, related to Figure 4**

(A) AvCAST RNA-guided *E.coli* genomic insertions at 10 targeted loci. Representative data for LE junction amplification are shown. (B) Insertion frequency for 36 targeted loci (AvPSP2 - 37) quantified by ddPCR. Data are represented as mean  $\pm$  SD (C) Type I-B subtype1 AvCAST RNA-guided insertion positions on 36 targeted loci by deep sequencing. Both RE and LE junctions were sequenced and representative insertion reads at each position measured by LE junction data are provided. Insertion at PSPs indicated in red were below the limit of detection (few or no insertion reads). (D) Comparison of insertion frequency between pSC101 and pBluescript donors. Data are represented as mean  $\pm$  SD (E) TTISS analysis of three representative loci (AvPSP2, AvPSP7, and AvPSP12) to test insertion specificity of AvCAST. Reads are mapped on CP001509 *E.coli* BL21(DE3) complete genome.

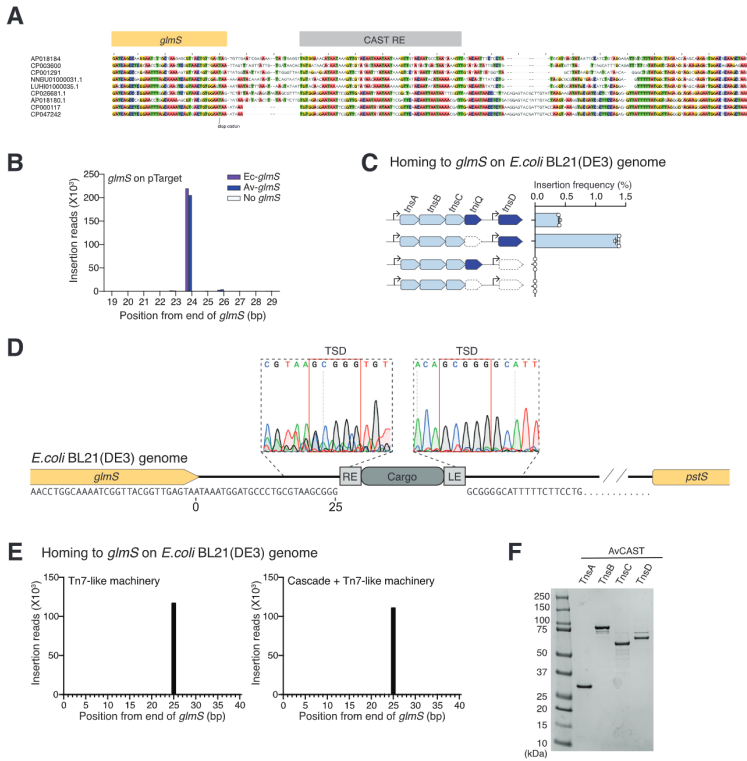


**Figure S5. Type I-B subtype1 AvCAST system homes to *glmS*, related to Figure 5**

(A) Alignment of CAST-IB1 loci at the insertion site. Ends of *glmS* are highlighted in orange while the CAST left end (LE) is shown in gray. Only 2 identical contigs have the transposon inserted 5-bp downstream of *glmS* while all other transposons are inserted about 24-bp downstream of the homing target site. (B) Deep sequencing reads showing Tn7-like machinery of AvCAST mediates a single prominent insertion at *glmS* Tn7 attachment site on plasmids. Purple bar indicates the insertion position on the plasmid harboring *E. coli glmS*. Blue bar indicates the insertion position on the plasmid harboring *A. variabilis glmS*. (C) Tn7-like machinery-mediated insertion frequency at the *glmS* gene on the *E. coli* BL21(DE3) genome in the absence of TnIQ, TnsD, or both. Data are represented as mean  $\pm$  SD (D) Sanger sequencing chromatograms for RE and LE junctions of insertion at the endogenous *glmS* Tn7 attachment site on *E. coli* BL21(DE3) genome. "GCGGG" is target site duplication as a signature of Tn7-like transposition. (E) AvCAST-mediated single prominent insertion at the endogenous *glmS* Tn7 attachment site on *E. coli* BL21(DE3) genome identified by deep sequencing. Left: with all Tn7-like machinery of AvCAST; right: with all AvCAST proteins including TnIQ and Cascade proteins. (F) Purified Tn7-like machinery components of AvCAST on Coomassie Brilliant Blue stained SDS-PAGE gel.

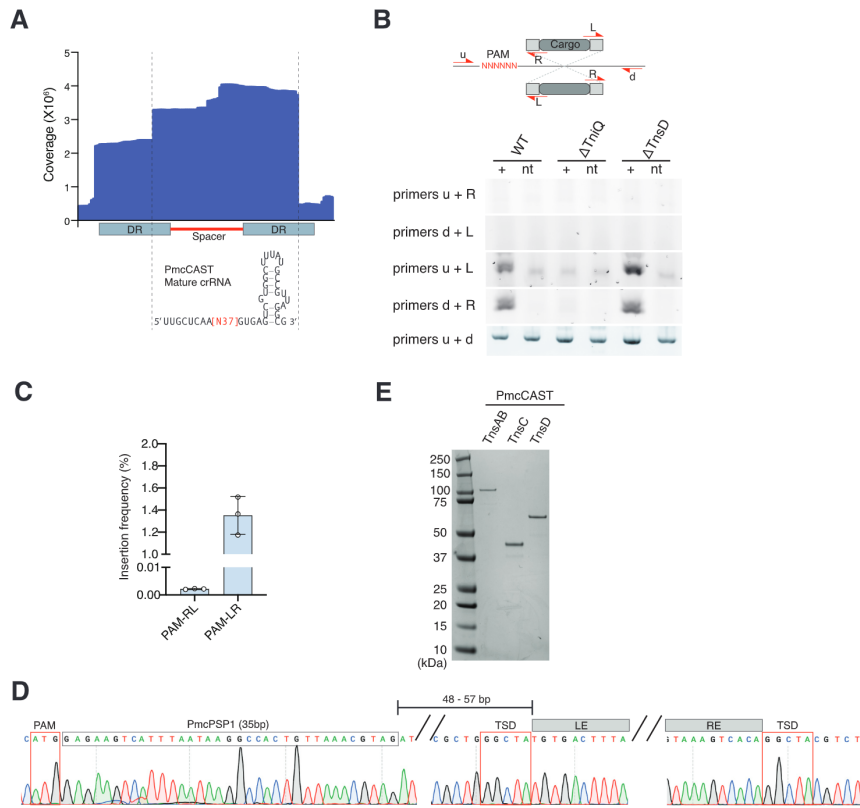


**Figure S6. Characterization of type I-B subtype2 PmcCAST, related to Figure 6**

(A) RNA sequence reads mapping to the minimal CRISPR array showing the mature crRNA sequence of PmcCAST. (B) Insertion directionality assayed by diagnostic PCR of plinsert on 6N PAM library plasmid with different primer pairs in  $\Delta$ TniQ or  $\Delta$ TnsD conditions. (C) Quantification of insertion frequency across the LE and RE junctions by ddPCR. Data are represented as mean  $\pm$  SD (D) Sanger sequencing chromatograms of a representative plinsert. PAM, PmcPSP1, TSDs, transposon ends are annotated. (E) Coomassie Brilliant Blue stained SDS-PAGE gel for purified Tn7-like machinery components of PmcCAST.

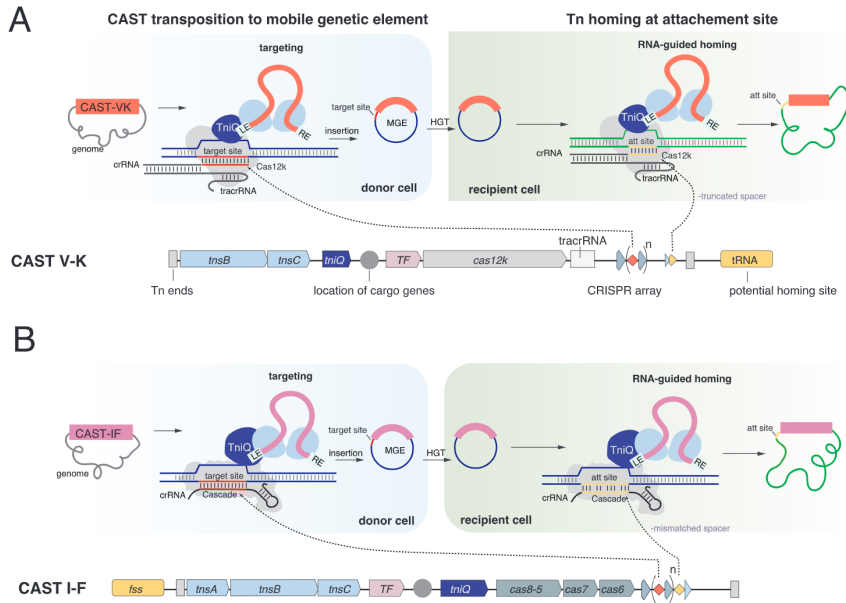


**Figure S7. Models comparing CAST V-K and CAST I-F, related to Figure 7**

Prototypical locus organization of CAST V-K systems and CAST I-F systems and models for CAST transposition to mobile element (donor cell in blue) and CAST homing transposition to bacterial chromosome (recipient cell in green). The loci are delimited by transposon ends (Tn ends, indicated as light vertical rectangles). Transposon core components (*tnsA*, *tnsB*, and *tnsC* in CAST I-F; *tnsB* and *tnsC* in CAST V-K) are colored in light blue while *tniQ* is colored in dark blue. Cas components (Cascade I-F and *cas12k*) are shown in gray. Conserved transcription factors (TF) are shown in pink. Locations of cargo genes are indicated with dark gray circles. CRISPR arrays are shown as gray triangles for the repeats, and red diamonds for the spacers. In CAST V-K the delocalized crRNA is indicated by a lighter triangle (partial repeat), and a truncated orange diamond (short spacer). In CAST I-F the homing spacer (targeting the homing target site) is indicated as a light orange diamond located at the distal spacer of the CRISPR-array. Homing target genes are colored in large yellow rectangles. Horizontal light gray triangle indicates the *tracrRNA* in the CAST V-K locus. CAST transposition to mobile genetic elements is mediated by the Cas effector machinery (I-F Cascade and crRNA or *Cas12k*, *tracrRNA*, and crRNA) which recognizes the target site (red) with RNA-guided targeting to insert the transposon using Tn components. For homing transposition, CAST V-K uses a dedicated crRNA (spacer in light orange) bearing a truncated spacer to target the homing site while CAST I-F uses a dedicated spacer, either located at the distal region of the CRISPR array or delocalized, to target the homing target site often with numerous mismatches between spacer and target (Petassi et al. 2020).